Figure 5 Relative gene expression levels of Oct4, Sox2, and Nanog in human fibroblasts, keratinocytes, CD133^{+} cells from cord blood, and NSCs. The relative gene expression levels in fibroblasts, keratinocytes, and CD133^{+} cells compared with hESCs were calculated from the data reported by Giorgetti *et al.*[85] and Page *et al.*[86] The relative gene expression levels in human NSCs compared with hESCs were used from the data reported by Kim *et al.*[13]

mouse fibroblasts leads to transdifferentiation of mouse fibroblasts into NSC-like cells, which can be subsequently reprogrammed into miPSCs by the transduction of Oct4.[74] The efficiency of miPSC generation was found to be 0.11% in their study.[74]

MOUSE CiPSC GENERATION USING SMALL-MOLECULE COCKTAILS

Hou *et al.* prepared miPSCs solely using a combination of seven small-molecule compounds that are chemically defined without using transduction or transfection of TFs.[17] It is difficult to select adequate small molecules that can replace the master regulatory gene Oct4. Therefore, Hou *et al.* first searched for small molecules that enabled MEF reprogramming in the absence of Oct4 using MEFs expressing Oct4 promoter-driven GFP to identify small molecules that facilitate cell reprogramming.[17] They identified FSK, 2-methyl-5-hydroxytryptamine, and D4476 as chemical substitutes for Oct4 after screening up to 10 000 small molecules, and they chose to use FSK as the chemical substitute of Oct4 in their research.[17] Because they had already developed the protocol to generate miPSCs using a small-molecule cocktail, 'VC6T' (VPA, CHIR99021, 616452, and tranylcypromine), with a single-gene transduction of Oct4,[15] they developed mouse CiPSCs using small-molecule cocktails in the absence of the transduction or transfection of small molecules. They used a four-step protocol to generate mouse CiPSCs (Figure 4f). (a) MEFs were first cultured with mESC medium containing VPA, CHIR99021, 616452, tranylcypromine, and FSK (VC6FT) for 16–20 days. (b) The

cells were then cultured with mESC medium containing VC6FT, 3-deazaneplanocin (DZNep, epigenetic modulator), and TTNPB (a synthetic retinoic acid receptor ligand). In these cells, the expression levels of most of the pluripotency marker genes were elevated but appeared to still be lower than those found in mESCs, which indicated a partially reprogrammed cell state. (c) In the third stage, the cells were cultured in mESC medium containing PD0325901 and CHIR99021 (2i medium), which promotes complete cellular reprogramming. (d) The colonies exhibiting mESC-like morphologies were shifted onto MEFs and cultured in mESC medium.[17] The reprogramming efficiency was as high as 0.2%.[17] CiPSCs prepared in this research resembled mESCs in terms of their gene expression profiles, epigenetic status, and potential for differentiation and germline transmission. This research suggests that exogenous 'master genes' are dispensable for generating miPSCs using small molecules. This chemical reprogramming strategy opens the door to generate functional, desirable cell types for clinical applications, provided we can succeed in generating human CiPSCs in the future.

SMALL MOLECULES CAN INDUCE HUMAN iPSCs IN COMBINATION WITH A FEW TFs

Small molecules successively promote the generation of miPSCs by reducing the numbers of TFs required, as shown in the previous section. Researchers started to investigate the generation of hiPSCs by reducing the numbers of TFs with the aid of small molecules. Figure 6 illustrates some schematic representations of the process of hiPSC generation from human somatic cells. Table 4 summarizes reported studies for human somatic cell reprogramming into hiPSCs by transduction with and without TFs in combination with small molecules. Only a few small molecules have been reported to promote reprogramming and/or to replace TFs during hiPSC generation compared with miPSC generation. These molecules for hiPSC generation include sodium butyrate (HDAC inhibitor), VPA (HDAC inhibitor), CHIR99021 (GSK3-β inhibitor), LiCl (GSK3-β inhibitor), 616452 (TGF-β inhibitor), SB431542 (TGF-β inhibitor), PD325901 (MEK inhibitor), N-oxaloylglycine (prolyl-4-hydroxylase inhibitor), PS48 (3-phosphoinositide-dependent protein kinase 1 activator), 8-Br-cAMP (cAMP-dependent protein kinase activator), fructose 2,6-bisphosphate (phosphofructokinase 1 activator), quercetin (hypoxia-inducible factor pathway activator), and 2,4-dinitrophenol (oxidative phosphorylation uncoupler; Table 2). It will be important to evaluate whether other small molecules that have biological activities in miPSC reprogramming are valid for use in hiPSC reprogramming.

Currently, the minimum transduction of Oct4 in combination with chemically defined small molecules is necessary to generate hiPSCs. This requirement is because the efficiency of hiPSC generation is much less than that of miPSC generation (eg, 0.0005–0.01%).
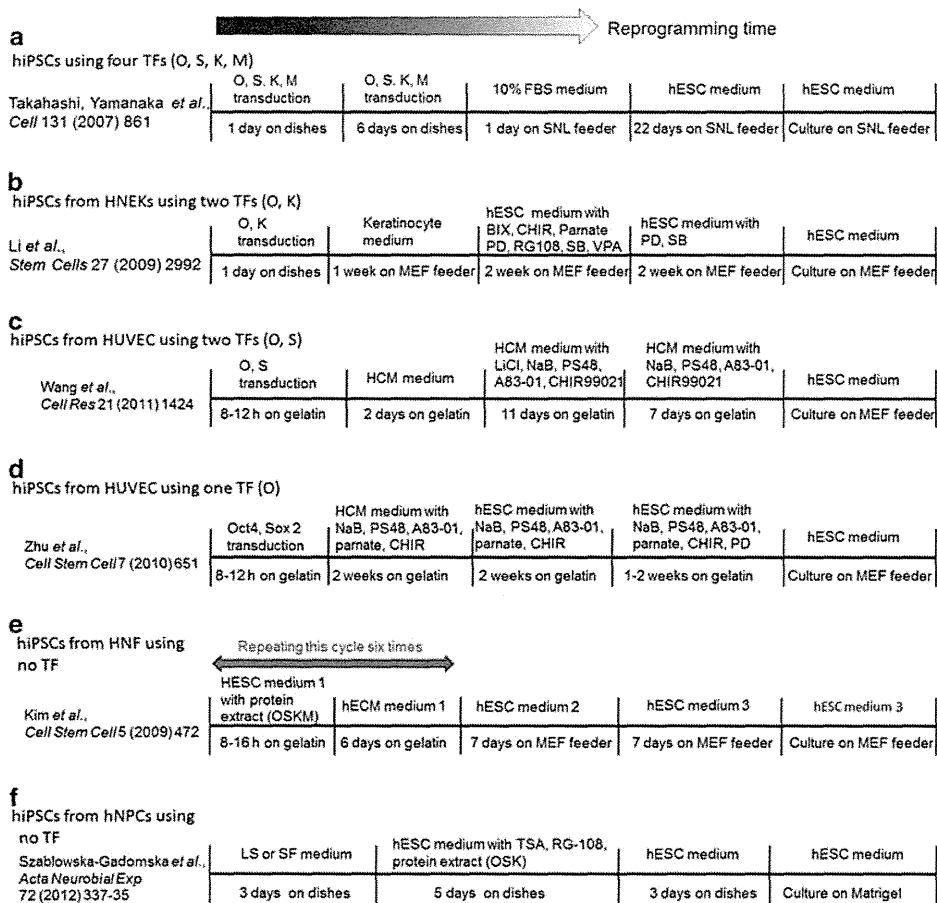
— 158 —

Reprogramming time

a
hiPSCs using four TFs (O, S, K, M)

Takahashi, Yamanaka et al.
Cell 131 (2007) 861

O, S. K, M transduction	O, S. K, M transduction	10% FBS medium	hESC medium	hESC medium
1 day on dishes	6 days on dishes	1 day on SNL feeder	22 days on SNL feeder	Culture on SNL feeder

b
hiPSCs from HNEKs using two TFs (O, K)

Li et al.,
Stem Cells 27 (2009) 2992

O, K transduction	Keratinocyte medium	hESC medium with BIX, CHIR, Parnate PD, RG108, SB, VPA	hESC medium with PD, SB	hESC medium
1 day on dishes	1 week on MEF feeder	2 week on MEF feeder	2 week on MEF feeder	Culture on MEF feeder

c
hiPSCs from HUVEC using two TFs (O, S)

Wang et al.,
Cell Res 21 (2011) 1424

O, S transduction	HCM medium	HCM medium with LiCl, NaB, PS48, A83-01, CHIR99021	HCM medium with NaB, PS48, A83-01, CHIR99021	hESC medium
8-12h on gelatin	2 days on gelatin	11 days on gelatin	7 days on gelatin	Culture on MEF feeder

d
hiPSCs from HUVEC using one TF (O)

Zhu et al.,
Cell Stem Cell 7 (2010) 651

Oct4, Sox2 transduction	HCM medium with NaB, PS48, A83-01, parnate, CHIR	hESC medium with NaB, PS48, A83-01, parnate, CHIR	hESC medium with NaB, PS48, A83-01, parnate, CHIR, PD	hESC medium
8-12h on gelatin	2 weeks on gelatin	2 weeks on gelatin	1-2 weeks on gelatin	Culture on MEF feeder

e
hiPSCs from HNF using no TF

Kim et al.,
Cell Stem Cell 5 (2009) 472

Repeating this cycle six times

HESC medium 1 with protein extract (OSKM)	hECM medium 1	hESC medium 2	hESC medium 3	hESC medium 3
8-16h on gelatin	6 days on gelatin	7 days on MEF feeder	7 days on MEF feeder	Culture on MEF feeder

f
hiPSCs from hNPCs using no TF

Szablowska-Gadomska et al.,
Acta Neurobial Exp
72 (2012) 337-35

LS or SF medium	hESC medium with TSA, RG-108, protein extract (OSK)	hESC medium	hESC medium
3 days on dishes	5 days on dishes	3 days on dishes	Culture on Matrigel

Figure 6 Schematic representation of hiPSC generation from human somatic cells by reducing the number of TFs with and without small molecules. (a) hiPSCs using four TFs (Oct4 [O], Sox2 [S], Klf4 [K], and c-Myc [M]);[8] (b) hiPSCs from human neonatal epidermal keratinocytes (HNEKs) using two TFs (O, K);[71] (c) hiPSCs from human umbilical vein endothelial cells (HUVECs) using two TFs (O, S);[70] (d) hiPSCs from HUVECs using one TF (O);[43] (e) hiPSCs from human newborn fibroblasts (HNFs) using no TFs;[18] and (f) hiPSCs from human NSCs using no TFs.[90] HCM medium indicates EndoGRO-VEGF complete medium (CHEMICON). LS and SF medium indicates low-serum and serum-free media, respectively. O, S, K, and M indicate the TFs Oct4, Sox2, Klf4, and c-Myc, respectively.

NSCs endogenously express *Sox2*, *Klf4*, and/or *c-Myc* to some extent, as was discussed in the previous section (Figure 5). Therefore, Kim et al. reprogrammed human fetal NSCs into hiPSCs by the transduction of only *Oct4*.[13] Their work suggests that only one TF, *OCT4*, should be sufficient to reprogram human fetal NSCs into hiPSCs. However, it is very difficult to obtain human fetal NSCs to generate patient-specific hiPSCs, and the efficiency of hiPSC generation is reported to be only 0.006% in their study.[13]

Zhu et al. developed their four-step protocol to generate hiPSCs from neonatal human epidermal keratinocytes, human umbilical vein endothelial cells (HUVECs), and amniotic-derived cells.[43] In the case of HUVEC-derived hiPSCs, the following protocol was used. (a) In the first stage, *Oct4* was transduced into cells cultured on gelatin-coated dishes for 8–12 h. (b) In the second stage, the cells were cultured in HUVEC medium containing sodium butyrate, PS48, A83-01, tranylcypromine, and CHIR99021 for 2 weeks on the gelatin. (c) In the third stage, the cells were cultured in hESC medium containing sodium butyrate, PS48, A83-01, tranylcypromine, and CHIR99021 for another 2 weeks on the gelatin. (d) In the fourth stage, the cells were cultured in hESC medium containing sodium butyrate, PS48, A83-01, tranylcypromine, CHIR99021, and PD0325901 for an additional 1–2 weeks on the gelatin to complete the full cellular reprogramming (Figure 6d). It was suggested that the single TF, *Oct4*, combined with a defined small-molecule cocktail is capable of reprogramming several human somatic cell types into hiPSCs that are functionally similar to pluripotent hESCs in terms of morphology, gene and protein expression, and differentiation capacity.[43] However, the reprogramming efficiency was extremely low (0.004%) because hiPSCs rather than miPSCs were generated.

Table 4 Reprogramming of human somatic cells into hiPSCs by transduction with and without TFs with the aid of small molecules

TFs required[a]	Somatic cells	PSCs	Small molecules	Efficiency (%)	Reference
Four factors					
OSKM	Human dermal fibroblasts	hiPSCs	None	0.02%	8
OSKM	hFFs	hiPSCs	RSC133	3 Times higher than control	82
Two factors					
OK	Human fetal NPCs	hiPSCs	None	0.006%	13
OS	Human cord blood-derived stem cells	hiPSCs	None	0.006%	64
OK	Human neonatal keratinocyte	hiPSCs	CHIR99021, Parnate (and PD0325901, SB431542)	0.005–0.01%	71
OK	Human neonetal epidermal keratinocytes	hiPSCs	A-83-01, PD032590, NaB, PS48 (+ Parnate, CHIR99021)	0.025%	43
OS	HUVEC	hiPSCs	A83, NaB, PS48, CHIR88021, LiCl	0.0015%	70
One factor					
O	Human fetal NPCs	hiPSCs	None	0.004%	13
O	Human neonetal epidermal keratinocytes	hiPSCs	A-83-01, PD032590, sodium butyrate, PS48 (+ Parnate, CHIR99021)	0.004%	43
O	HUVECs and amniotic fluid-derived cells	hiPSCs	A83-01, PD032590, NaB, PS48 (+ Parnate, CHIR99021)	0.0025–0.01%	43
O	HUVEC	hiPSCs	A83-01, NaB, PS48, LiCl, CHIR99021 (or PD0325901)	0.0005%	70

Abbreviations: hFF, human foreskin fibroblast; TF, transcription factor.
[a]O, S, K, and M indicate Oct4, Sox2, Klf-4, and c-Myc, respectively.

Wang et al. also generated hiPSCs using either one transduced factor (Oct4) or two transduced factors (Oct4 and Sox2) with the aid of small molecules.[70] They used small-molecule cocktails similar to those used by Zhu et al.[43] but also treated the cells with LiCl (5 mM) from days 3 to 18, which facilitated miPSC and hiPSC generation (Figure 6c).[70] hiPSC colonies were picked for expansion on feeder cells after approximately 1 month. The effect of LiCl on promoting reprogramming was only partially dependent on its major target, GSK-3β.[70] However, LiCl is unlike other GSK-3β inhibitors, as it enhances Nanog expression and also promotes its transcriptional activity. LiCl also works by promoting epigenetic modifications via the downregulation of an H3K4-specific histone demethylase, LSD1. However, the efficiency of hiPSC generation was still extremely low (0.0015 and 0.0005% for two-factor and one-factor transduction, respectively).

If hiPSCs can be generated from patient-specific cells and/ or different human leukocyte antigen (HLA) types of human somatic cells using only chemically defined small molecules with high efficiency (eg, preferentially >0.1%), the door would be opened for the potential use of hiPSCs in clinical applications. Currently, to our knowledge, hiPSC generation solely based on chemically defined small molecules has not yet been reported, although hiPSCs have been generated using cell extracts and/or proteins without the use of TFs.[18,58,90]

CONCLUSIONS AND PERSPECTIVES

Introduction of small and large molecules can target signaling transduction pathways and can affect DNA replication, cell differentiation, apoptosis, and the reprogramming of the cells into iPSCs. Several specific small molecules can successfully enhance the reprogramming efficiencies of mouse and human somatic cells into iPSCs. Since 2013, miPSCs have been generated via treatment with small molecules without the use of genetic material.[17,68] However, it is still challenging to generate hiPSCs by treating cells with only small molecules. The generation of human and mouse piPSCs using pluripotent proteins or cell extracts without the
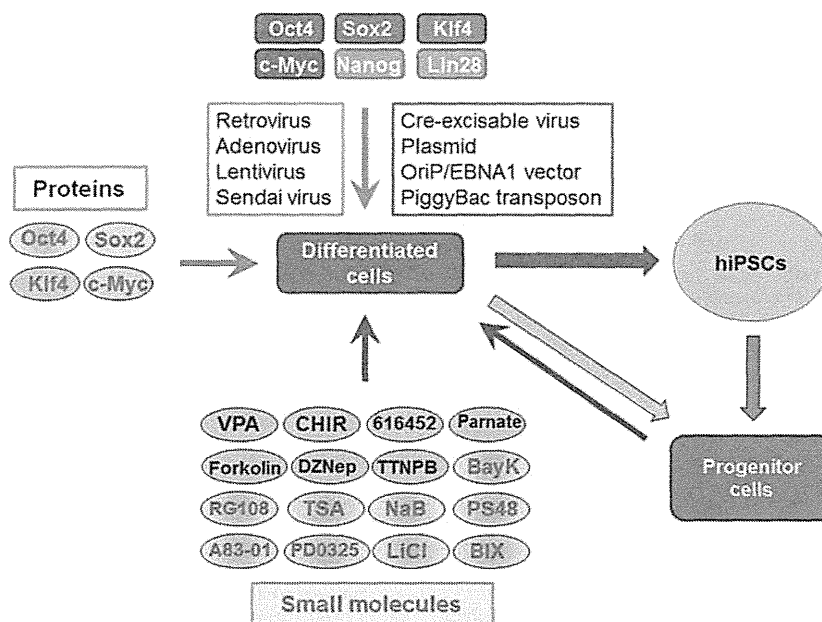
— 160 —

Figure 7 Schematic illustration of somatic cell reprogramming to iPSCs and progenitor or adult stem cells. Somatic cells can be reprogrammed to iPSCs using viral or non-viral introduction of exogenous TFs or protein transfection. Small molecules can either substitute for certain TFs and/or improve reprogramming efficiency by epigenetic modifications or signaling pathway regulation. The abbreviations of the small molecules are shown in Table 2.

use of genetic material has been reported.[18,21] However, currently, piPSCs are not a popular method for generating iPSCs, although more than 5 years has passed since the first reports of their generation. The hesitancy to adopt the method is likely due to the extremely low generation efficiency and the difficulty of preparing pluripotent proteins tagged with CPP. Figure 7 summarizes the reprogramming methods that have been developed and that may be promising in the future. Currently, target cells, such as dopamine-secreting cells, insulin-secreting β cells, and cardiomyocytes, may be prepared from PSCs as follows: (a) somatic cells from blood, fat tissue, or other sources of tissues are isolated; (b) the somatic cells are reprogrammed into iPSCs; and (c) iPSCs are differentiated into the targeted cells. In this case, which includes the use of hESCs and hiPSCs, it is extremely difficult to obtain highly pure populations of the target cells. Furthermore, it is impossible to avoid the potential for tumor generation when these targeted cells are transplanted into humans.[91] Therefore, we suggest that the direct reprogramming of somatic cells into progenitor (stem) cells, including adult stem cells, such as NSCs, cardiomyocyte progenitor cells, hepatocyte stem cells, hematopoietic stem cells, and mesenchymal stem cells, as an attractive alternative for clinical applications. It will be interesting to develop small molecules to guide human somatic cells into the transdifferentiation of tissue-specific progenitor cells or stem cells.[76,92–95] In this case, xeno-free cultures are much easier for culturing the progenitor cells compared with PSCs because MEFs are not required for the culturing of progenitor cells and adult stem cells. Although

NSCs are reported to be able to proliferate for more than 20–130 passages,[96–98] mesenchymal stem cells, such as adipose-derived stem cells and amniotic fluid stem cells, have limited proliferation capacities (eg, 8–12 passages). Therefore, the establishment of small molecules to extend the proliferation of adult stem cells and progenitor cells should be a priority in regenerative medicine. Because bone marrow stem cells and hematopoietic stem cells are ready to be used in clinical applications, the only obstacle to the use of these adult stem cells in clinical applications is their limited proliferation and their overall shortage, which leads to low numbers of clinical trials. The shortages of progenitor cells and adult stem cells can be addressed by reprogramming somatic cells into progenitor cells and adult stem cells using small molecules, which do not disrupt or interrupt host cell genomes. The development of small molecules to guide human somatic cells into progenitor cells, adult stem cells, and iPSCs will open avenues for the clinical application of these types of progenitor cells and stem cells.[65,99,100]

DISCLOSURE/CONFLICT OF INTEREST

The authors declare no conflict of interest.

1. Fujimoto M, Hayashi H, Takagi Y, *et al*. Transplantation of telencephalic neural progenitors induced from embryonic stem cells into subacute phase of focal cerebral ischemia. Lab Invest 2012;92:522–531.
2. Callahan LA, Xie S, Barker IA, *et al*. Directed differentiation and neurite extension of mouse embryonic stem cell on aligned poly(lactide) nanofibers functionalized with YIGSR peptide. Biomaterials 2013;34: 9089–9095.
3. Higuchi A, Ling QD, Kumar SS, *et al*. Design of polymeric materials for culturing human pluripotent stem cells: progress toward feeder-free and xeno-free culturing. Prog Polym Sci 2014;39:1348–1374.
4. Gokhale PJ, Andrews PW. Human embryonic stem cells: 10 years on. Lab Invest 2009;89:259–262.
5. Hankowski KE, Hamazaki T, Umezawa A, *et al*. Induced pluripotent stem cells as a next-generation biomedical interface. Lab Invest 2011;91:972–977.
6. de Wert G, Mummery C. Human embryonic stem cells: research, ethics and policy. Hum Reprod 2003;18:672–682.
7. Takahashi K, Yamanaka S. Induction of pluripotent stem cells from mouse embryonic and adult fibroblast cultures by defined factors. Cell 2006;126:663–676.
8. Takahashi K, Tanabe K, Ohnuki M, *et al*. Induction of pluripotent stem cells from adult human fibroblasts by defined factors. Cell 2007;131: 861–872.
9. Okita K, Ichisaka T, Yamanaka S. Generation of germline-competent induced pluripotent stem cells. Nature 2007;448:313–317.
10. Aoi T, Yae K, Nakagawa M, *et al*. Generation of pluripotent stem cells from adult mouse liver and stomach cells. Science 2008;321:699–702.
11. Yu J, Vodyanik MA, Smuga-Otto K, *et al*. Induced pluripotent stem cell lines derived from human somatic cells. Science 2007;318:1917–1920.
12. Nakagawa M, Koyanagi M, Tanabe K, *et al*. Generation of induced pluripotent stem cells without Myc from mouse and human fibroblasts. Nat Biotechnol 2008;26:101–106.
13. Kim JB, Greber B, Arauzo-Bravo MJ, *et al*. Direct reprogramming of human neural stem cells by OCT4. Nature 2009;461:649–653.
14. Xie M, Cao N, Ding S. Small molecules for cell reprogramming and heart repair: Progress and perspective. Acs Chem Biol 2014;9:34–44.
15. Li Y, Zhang Q, Yin X, *et al*. Generation of iPSCs from mouse fibroblasts with a single gene, Oct4, and small molecules. Cell Res 2011;21: 196–204.
16. Kim JB, Sebastiano V, Wu GM, *et al*. Oct4-induced pluripotency in adult neural stem cells. Cell 2009;136:411–419.
17. Hou PP, Li YQ, Zhang X, *et al*. Pluripotent stem cells induced from mouse somatic cells by small-molecule compounds. Science 2013;341:651–654.
18. Kim D, Kim CH, Moon JI, *et al*. Generation of human induced pluripotent stem cells by direct delivery of reprogramming proteins. Cell Stem Cell 2009;4:472–476.
19. Zhou H, Wu S, Joo JY, *et al*. Generation of induced pluripotent stem cells using recombinant proteins. Cell Stem Cell 2009;4:381–384.
20. Li WL, Ding S. Small molecules that modulate embryonic stem cell fate and somatic cell reprogramming. Trends Pharmacol Sci 2010;31:36–45.
21. Yamanaka S. Strategies and new developments in the generation of patient-specific pluripotent stem cells. Cell Stem Cell 2007;1:39–49.
22. Cohen DE, Melton D. Turning straw into gold: directing cell fate for regenerative medicine. Nat Rev Genet 2011;12:243–252.
23. Chun YS, Chaudhari P, Jang YY. Applications of patient-specific induced pluripotent stem cells; Focused on disease modeling, drug screening and therapeutic potentials for liver disease. Int J Biol Sci 2010;6:796–805.
24. Nishimura K, Sano M, Ohtaka M, *et al*. Development of defective and persistent Sendai virus vector: a unique gene delivery/expression system ideal for cell reprogramming. J Biol Chem 2011;286:4760–4771.
25. Stadtfeld M, Nagaya M, Utikal J, *et al*. Induced pluripotent stem cells generated without viral integration. Science 2008;322:945–949.
26. Zhou WB, Freed CR. Adenoviral gene delivery can reprogram human fibroblasts to induced pluripotent stem cells. Stem Cells 2009;27: 2667–2674.
27. Woltjen K, Michael IP, Mohseni P, *et al*. piggyBac transposition reprograms fibroblasts to induced pluripotent stem cells. Nature 2009;458:766–770.
28. Okita K, Nakagawa M, Hyenjong H, *et al*. Generation of mouse induced pluripotent stem cells without viral vectors. Science 2008;322: 949–953.
29. Si-Tayeb K, Noto FK, Sepac A, *et al*. Generation of human induced pluripotent stem cells by simple transient transfection of plasmid DNA encoding reprogramming factors. BMC. Develop Biol 2010;10:81.
30. Yu J, Hu K, Smuga-Otto K, *et al*. Human induced pluripotent stem cells free of vector and transgene sequences. Science 2009;324:797–801.
31. Kaji K, Norrby K, Paca A, *et al*. Virus-free induction of pluripotency and subsequent excision of reprogramming factors. Nature 2009;458: 771–775.
32. MacArthur CC, Fontes A, Ravinder N, *et al*. Generation of human-induced pluripotent stem cells by a nonintegrating RNA sendai virus vector in feeder-free or xeno-free conditions. Stem Cells Int 2012; 2012:564612.
33. Chou BK, Mali P, Huang XS, *et al*. Efficient human iPS cell derivation by a non-integrating plasmid from blood cells with unique epigenetic and gene expression signatures. Cell Res 2011;21:518–529.
34. Cheng L, Hansen NF, Zhao L, *et al*. Low incidence of DNA sequence variation in human induced pluripotent stem cells generated by nonintegrating plasmid expression. Cell Stem Cell 2012;10:337–344.
35. Lin SL, Chang DC, Chang-Lin S, *et al*. Mir-302 reprograms human skin cancer cells into a pluripotent ES-cell-like state. RNA 2008;14: 2115–2124.
36. Soldner F, Hockemeyer D, Beard C, *et al*. Parkinson's disease patient-derived induced pluripotent stem cells free of viral reprogramming factors. Cell 2009;136:964–977.
37. Warren L, Manos PD, Ahfeldt T, *et al*. Highly efficient reprogramming to pluripotency and directed differentiation of human cells with synthetic modified mRNA. Cell Stem Cell 2010;7:618–630.
38. Firestone AJ, Chen JK. Controlling destiny through chemistry: Small-molecule regulators of cell fate. Acs Chem Biol 2010;5:15–34.
39. Wu YL, Pandian GN, Ding YP, *et al*. Clinical grade iPS cells: Need for versatile small molecules and optimal cell sources. Chem Biol 2013;20:1311–1322.
40. Zhu S, Wei W, Ding S. Chemical strategies for stem cell biology and regenerative medicine. Annu Rev Biomed Eng 2011;13:73–90.
41. Feng B, Ng JH, Heng JCD, *et al*. Molecules that promote or enhance reprogramming of somatic cells to induced pluripotent stem cells. Cell Stem Cell 2009;4:301–312.
42. Huangfu D, Maehr R, Guo W, *et al*. Induction of pluripotent stem cells by defined factors is greatly improved by small-molecule compounds. Nat Biotechnol 2008;26:795–797.
43. Zhu SY, Li WL, Zhou HY, *et al*. Reprogramming of human primary somatic cells by OCT4 and chemical compounds. Cell Stem Cell 2010;7:651–655.
44. Zhang XZ. Modulation of embryonic stem cell fate and somatic cell reprogramming by small molecules. Reprod Biomed Online 2010;21: 26–36.
45. Anastasia L, Pelissero G, Venerando B, *et al*. Cell reprogramming: expectations and challenges for chemistry in stem cell biology and regenerative medicine. Cell Death Differ 2010;17:1230–1237.
46. Li WL, Jiang K, Ding S. Concise review: A chemical approach to control cell fate and function. Stem Cells 2012;30:61–68.
47. Lu JY, Kong XQ, Luo C, *et al*. Application of epigenome-modifying small molecules in induced pluripotent stem cells. Med Res Rev 2013;33:790–822.
48. Lukaszewicz AI, McMillan MK, Kahn M. Small molecules and stem cells. Potency and lineage commitment: The new quest for the fountain of youth. J Med Chem 2010;53:3439–3453.
49. Groß B, Sgodda M, Rasche M, *et al*. Improved generation of patient-specific induced pluripotent stem cells using a chemically-defined and matrigel-based approach. Curr Mol Med 2013;13:765–776.
50. Wadia JS, Dowdy SF. Protein transduction technology. Curr Opin Biotech 2002;13:52–56.

51. Michiue H, Tomizawa K, Wei FY, *et al*. The NH2 terminus of influenza virus hemagglutinin-2 subunit peptides enhances the antitumor potency of polyarginine-mediated p53 protein transduction. J Biol Chem 2005;280:8285–8289.

52. Inoue M, Tomizawa K, Matsushita M, *et al*. p53 protein transduction therapy: Successful targeting and inhibition of the growth of the bladder cancer cells. Eur Urol 2006;49:161–168.

53. Lafevre-Bernt M, Wu S, Lin X. Recombinant, refolded tetrameric p53 and gonadotropin-releasing hormone-p53 slow proliferation and induce apoptosis in p53-deficient cancer cells. Mol Cancer Ther 2008;7:1420–1429.

54. Ziegler A, Nervi P, Durrenberger M, *et al*. The cationic cell-penetrating peptide CPP(TAT) derived from the HIV-1 protein TAT is rapidly transported into living fibroblasts: optical, biophysical, and metabolic evidence. Biochemistry 2005;44:138–148.

55. El-Sayed A, Futaki S, Harashima H. Delivery of macromolecules using arginine-rich cell-penetrating peptides: ways to overcome endosomal entrapment. Aaps J 2009;11:13–22.

56. Jin J, Kwon YW, Paek JS, *et al*. Analysis of differential proteomes of induced pluripotent stem cells by protein-based reprogramming of fibroblasts. J Proteome Res 2011;10:977–989.

57. Zhu XQ, Pan XH, Wang WB, *et al*. Transient in vitro epigenetic reprogramming of skin fibroblasts into multipotent cells. Biomaterials 2010;31:2779–2787.

58. Zheng Z, Jian J, Zhang XL, *et al*. Reprogramming of human fibroblasts into multipotent cells with a single ECM proteoglycan, fibromodulin. Biomaterials 2012;33:5821–5831.

59. Cho HJ, Lee CS, Kwon YW, *et al*. Induction of pluripotent stem cells from adult somatic cells by protein-based reprogramming without genetic manipulation. Blood 2010;116:386–395.

60. Rajasingh J, Lambers E, Hamada H, *et al*. Cell-free embryonic stem cell extract-mediated derivation of multipotent stem cells from NIH3T3 fibroblasts for functional and anatomical ischemic tissue repair. Circ. Res. 2008;102:E107–E117.

61. Rhee YH, Ko JY, Chang MY, *et al*. Protein-based human iPS cells efficiently generate functional dopamine neurons and can treat a rat model of Parkinson disease. J Clinical Invest 2011;121:2326–2335.

62. Vezoli J. Recombinant proteins to induce pluripotent stem cells: Promises for a safer and thriving step toward clinical trials. Movement Disord 2011;26:1409–1409.

63. Shi Y, Desponts C, Do JT, *et al*. Induction of pluripotent stem cells from mouse embryonic fibroblasts by Oct4 and Klf4 with small-molecule compounds. Cell Stem Cell 2008;3:568–574.

64. Giorgetti A, Montserrat N, Aasen T, *et al*. Generation of induced pluripotent stem cells from human cord blood using OCT4 and SOX2. Cell Stem Cell 2009;5:353–357.

65. Jung DW, Kim WH, Williams DR. Reprogram or reboot: Small molecule approaches for the production of induced pluripotent stem cells and direct cell reprogramming. Acs Chem Biol 2014;9:80–95.

66. Sterneckert J, Hoing S, Scholer HR. Concise review: Oct4 and more: The reprogramming expressway. Stem Cells 2012;30:15–21.

67. Shi Y, Do JT, Desponts C, *et al*. A combined chemical and genetic approach for the generation of induced pluripotent stem cells. Cell Stem Cell 2008;2:525–528.

68. Pasha Z, Haider HK, Ashraf M. Efficient non-viral reprogramming of myoblasts to stemness with a single small molecule to generate cardiac progenitor cells. PLoS One 2011;6:e23667.

69. Ichida JK, Blanchard J, Lam K, *et al*. A small-molecule inhibitor of tgf-Beta signaling replaces sox2 in reprogramming by inducing nanog. Cell Stem Cell 2009;5:491–503.

70. Wang Q, Xu XX, Li J, *et al*. Lithium, an anti-psychotic drug, greatly enhances the generation of induced pluripotent stem cells. Cell Res 2011;21:1424–1435.

71. Li W, Zhou H, Abujarour R, *et al*. Generation of human-induced pluripotent stem cells in the absence of exogenous Sox2. Stem Cells 2009;27:2992–3000.

72. Staerk J, Lyssiotis CA, Medeiro LA, *et al*. Pan-Src family kinase inhibitors replace Sox2 during the direct reprogramming of somatic cells. Angew Chem Int Edit 2011;50:5733–5735.

73. Yuan X, Wan HF, Zhao XY, *et al*. Brief report: Combined chemical treatment enables Oct4-induced reprogramming from mouse embryonic fibroblasts. Stem Cells 2011;29:549–553.

74. Moon JH, Heo JS, Kim JS, *et al*. Reprogramming fibroblasts into induced pluripotent stem cells with Bmi1. Cell Res 2011;21:1305–1315.

75. Lyssiotis CA, Foreman RK, Staerk J, *et al*. Reprogramming of murine fibroblasts to induced pluripotent stem cells with chemical complementation of Klf4. Proc Natl Acad Sci USA 2009;106:8912–8917.

76. Allsopp TE, Bunnage ME, Fish PV. Small molecule modulation of stem cells in regenerative medicine: recent applications and future direction. Medchemcomm 2010;1:16–29.

77. Mikkelsen TS, Hanna J, Zhang XL, *et al*. Dissecting direct reprogramming through integrative genomic analysis. Nature 2008;454:49–55.

78. Lee MG, Wynder C, Schmidt DM, *et al*. Histone H3 lysine 4 demethylation is a target of nonselective antidepressive medications. Chem Biol 2006;13:563–567.

79. Mali P, Chou BK, Yen J, *et al*. Butyrate greatly enhances derivation of human induced pluripotent stem cells by promoting epigenetic remodeling and the expression of pluripotency-Associated genes. Stem Cells 2010;28:713–720.

80. Liang GY, Taranova O, Xia K, *et al*. Butyrate promotes induced pluripotent stem cell generation. J Biol Chem 2010;285:25516–25521.

81. Yoshida Y, Takahashi K, Okita K, *et al*. Hypoxia enhances the generation of induced pluripotent stem cells. Cell Stem Cell 2009;5:237–241.

82. Lee J, Xia Y, Son MY, *et al*. A novel small molecule facilitates the reprogramming of human somatic cells into a pluripotent state and supports the maintenance of an undifferentiated state of human pluripotent stem cells. Angew Chem Int Edit 2012;51:12509–12513.

83. Chen TT, Shen L, Yu J, *et al*. Rapamycin and other longevity-promoting compounds enhance the generation of mouse induced pluripotent stem cells. Aging Cell 2011;10:908–911.

84. Li ZH, Rana TM. A kinase inhibitor screen identifies small-molecule enhancers of reprogramming and iPS cell generation. Nat Commun 2012;3:2059.

85. Giorgetti A, Montserrat N, Rodriguez-Piza I, *et al*. Generation of induced pluripotent stem cells from human cord blood cells with only two factors: Oct4 and Sox2. Nat Protoc 2010;5:811–820.

86. Page RL, Ambady S, Holmes WF, *et al*. Induction of stem cell gene expression in adult human fibroblasts without transgenes. Cloning Stem Cells 2009;11:417–426.

87. Kim JB, Zaehres H, Wu GM, *et al*. Pluripotent stem cells induced from adult neural stem cells by reprogramming with two factors. Nature 2008;454:646–650.

88. Silva J, Barrandon O, Nichols J, *et al*. Promotion of reprogramming to ground state pluripotency by signal inhibition. PLoS Biol 2008;6:e253.

89. Huangfu D, Osafune K, Maehr R, *et al*. Induction of pluripotent stem cells from primary human fibroblasts with only Oct4 and Sox2. Nat Biotechnol 2008;26:1269–1275.

90. Szablowska-Gadomska I, Sypecka J, Zayat V, *et al*. Treatment with small molecules is an important milestone towards the induction of pluripotency in neural stem cells derived from human cord blood. Acta Neurobiol Exp 2012;72:337–350.

91. Higuchi A, Ling QD, Chang Y, *et al*. Physical cues of biomaterials guide stem cell differentiation fate. Chem Rev 2013;113:3297–3328.

92. Masip M, Veiga A, Belmonte JCI, *et al*. Reprogramming with defined factors: from induced pluripotency to induced transdifferentiation. Mol Hum Reprod 2010;16:856–868.

93. Efe JA, Ding S. The evolving biology of small molecules: controlling cell fate and identity. Philos T R Soc B 2011;366:2208–2221.

94. Roessler R, Boddeke E, Copray S. Induced pluripotent stem cell technology and direct conversion: New possibilities to study and treat Parkinson's disease. Stem Cell Rev Rep 2013;9:505–513.

95. Masuda S, Wu J, Hishida T, *et al*. Chemically induced pluripotent stem cells (CiPSCs): a transgene-free approach.. J Mol Cell Biol 2013;5:354–355.

96. Han DW, Tapia N, Hermann A, *et al*. Direct reprogramming of fibroblasts into neural stem cells by defined factors. Cell Stem Cell 2012;10:465–472.

97. Lujan E, Chanda S, Ahlenius H, *et al*. Direct conversion of mouse fibroblasts to self-renewing, tripotent neural precursor cells. Proc Natl Acad Sci USA 2012;109:2527–2532.

98. Thier M, Worsdorfer P, Lakes YB, *et al*. Direct conversion of fibroblasts into stably expandable neural stem cells. Cell Stem Cell 2012;10:473–479.

99. Tapia N, Han DW, Scholer HR. Restoring stem cell function in aged tissues by direct reprogramming? Cell Stem Cell 2012;10:653–656.

100. Li WL, Jiang K, Wei WG, *et al*. Chemical approaches to studying stem cell biology. Cell Res 2013;23:81–91.

Role of Notch Signaling in the Maintenance of Human Mesenchymal Stem Cells Under Hypoxic Conditions

Hiroyuki Moriyama,[1,*] Mariko Moriyama,[1,*] Haruki Isshi,[1] Shin Ishihara,[1] Hanayuki Okura,[2] Akihiro Ichinose,[3] Toshiyuki Ozawa,[4] Akifumi Matsuyama,[2] and Takao Hayakawa[1]

Human adipose tissue-derived multilineage progenitor cells (hADMPCs) are attractive for cell therapy and tissue engineering because of their multipotency and ease of isolation without serial ethical issues. However, their limited in vitro lifespan in culture systems hinders their therapeutic application. Some somatic stem cells, including hADMPCs, are known to be localized in hypoxic regions; thus, hypoxia may be beneficial for ex vivo culture of these stem cells. These cells exhibit a high level of glycolytic metabolism in the presence of high oxygen levels and further increase their glycolysis rate under hypoxia. However, the physiological role of glycolytic activation and its regulatory mechanisms are still incompletely understood. Here, we show that Notch signaling is required for glycolysis regulation under hypoxic conditions. Our results demonstrate that 5% O_2 dramatically increased the glycolysis rate, improved the proliferation efficiency, prevented senescence, and maintained the multipotency of hADMPCs. Intriguingly, these effects were not mediated by hypoxia-inducible factor (HIF), but rather by the Notch signaling pathway. Five percent O_2 significantly increased the level of activated Notch1 and expression of its downstream gene, HES1. Furthermore, 5% O_2 markedly increased glucose consumption and lactate production of hADMPCs, which decreased back to normoxic levels on treatment with a γ-secretase inhibitor. We also found that HES1 was involved in induction of GLUT3, TPI, and PGK1 in addition to reduction of TIGAR and SCO2 expression. These results clearly suggest that Notch signaling regulates glycolysis under hypoxic conditions and, thus, likely affects the cell lifespan via glycolysis.

Introduction

HUMAN ADIPOSE TISSUE-DERIVED mesenchymal stem cells (MSCs), also referred to as human adipose tissue-derived multilineage progenitor cells (hADMPCs), are multipotent stem cells that can differentiate into various types of cells, including hepatocytes [1], cardiomyoblasts [2], pancreatic cells [3], and neuronal cells [4–6]. They can be easily and safely obtained from lipoaspirate without posing serious ethical issues and can also be expanded ex vivo under appropriate culture conditions. Moreover, MSCs, including hADMPCs, have the ability to migrate to injured areas and secrete a wide variety of cytokines and growth factors that are necessary for tissue regeneration [7–11]. In addition, due to their hypoimmunogenicity and immunomodulatory effects, hADMPCs are good candidates as gene delivery vehicles for therapeutic purposes [12]. Thus, hADMPCs are attractive seeding cells for cell therapy and tissue engineering. However, similar to other somatic stem cells or primary cells,

hADMPCs have limited growth potential and ultimately stop proliferation as a result of cellular senescence [13], which hinders their therapeutic application.

Conversely, embryonic stem cells (ESCs) and induced pluripotent stem cells (iPSCs) are immortal under standard culture conditions. Recently, several groups have reported that these cells greatly rely on glycolysis for energy production even under high-oxygen conditions [14–16]. This phenomenon is known as the Warburg effect and was originally described for cancer cells by Otto Warburg in the 1920s [17]. Although mitochondrial respiration is more efficient than glycolysis in generating ATP (net yield of 30 ATPs vs. 2 ATPs), glycolysis is able to produce ATP considerably faster than mitochondrial respiration as long as glucose supplies are adequate. Thus, a metabolic shift from mitochondrial respiration to glycolysis would provide a growth advantage for actively proliferating cells. Moreover, Kondoh et al. demonstrated that enhanced glycolysis is also involved in cellular immortalization through reduction of

[1]Pharmaceutical Research and Technology Institute, Kinki University, Higashi-Osaka, Osaka, Japan.
[2]Platform of Therapeutics for Rare Disease and Health Policy, National Institute of Biomedical Innovation, Kobe, Japan.
[3]Department of Plastic Surgery, Kobe University Hospital, Kobe, Japan.
[4]Department of Dermatology, Graduate School of Medicine, Osaka City University, Osaka, Japan.
*These two authors contributed equally to this work.

intrinsic reactive oxygen species (ROS) production [14,18,19]. Since accumulation of intrinsic ROS levels could be a major reason for replicative senescence [20], enhancing glycolysis in cultured cells might improve the quality of the cells by suppressing premature senescence. One candidate method for induction of glycolysis is application of low-oxygen conditions to activate the transcription factor, hypoxia-inducible factor (HIF). HIF-1 is known to increase the expression of most glycolytic enzymes and the glucose transporters GLUT1 and GLUT3 [20]. Thus, several studies have reported that hypoxia is beneficial for the maintenance of hESCs in a pluripotent state [21,22]. Moreover, low oxygen tension has been reported to enhance the generation of iPSCs both from mouse and human primary fibroblasts [23].

Recently, hypoxic culture conditions have also been reported to confer a growth advantage, prevent premature senescence, and maintain undifferentiated states in somatic stem cells; for example, hematopoietic stem cells (HSCs) [24], neural stem cells [25], and bone marrow-derived MSCs [26]. These stem cells reside in their local microenvironments called the "stem cell niche," where the oxygen tension is relatively low (in the range of 1%–9%). Thus, hypoxic culture may be beneficial to these stem cells with regard to in vitro proliferation, cell survival, and differentiation. Takubo et al. reported that HSCs activated Pdk through HIF1α in hypoxic culture conditions, resulting in maintenance of glycolytic flow and suppression of the influx of glycolytic metabolites into mitochondria, and this glycolytic metabolic state was shown to be indispensable for the maintenance of HSCs [27]. Several studies have reported that MSCs exhibit a high level of glycolytic metabolism in the presence of high oxygen levels and further increase their rate of glycolysis on culture under hypoxia [28,29]. However, a relationship between beneficial effects of hypoxic conditions and metabolic status in addition to involvement of HIFs in the metabolic changes has not been investigated in these reports.

In this study, we aimed at investigating the effect of 5% oxygen on hADMPCs. Our results demonstrate that culture under 5% oxygen increased the glycolysis rate, improved the proliferation efficiency, prevented the cellular senescence, and maintained the undifferentiated status of hADMPCs. Intriguingly, these effects were not mediated by HIF, but rather by Notch signaling, an important signaling pathway required for the development of many cell types and maintenance of stem cells [30,31]. Five percent oxygen activated Notch signaling, resulting in the upregulation of *SLC2A3*, *TPI*, and *PGK1* in addition to the downregulation of *TIGAR* and *SCO2*, which may contribute to the increase in the glycolysis rate. These observations, thus, provide new regulatory mechanisms for stemness maintenance obtained under 5% oxygen conditions.

Materials and Methods

Adipose tissue samples

Subcutaneous adipose tissue samples (10–50 g each) were resected during plastic surgery from five female and two male patients (age 20–60 years) as discarded tissue. The study protocol was approved by the Review Board for Human Research of Kobe University Graduate School of Medicine Foundation for Biomedical Research and Innovation, Osaka City University Graduate School of Medicine, and Kinki University Pharmaceutical Research and Technology Institute (reference number: 12-043). Each subject provided signed informed consent.

Cell culture

hADMPCs were isolated as previously reported [11,32–34] and maintained in a medium containing 60% DMEM low glucose, 40% MCDB-201 medium (Sigma Aldrich), 1× insulin-transferrin-selenium (Life Technologies), 1 nM dexamethasone (Sigma Aldrich), 100 mM ascorbic acid 2-phosphate (Wako), 10 ng/mL epidermal growth factor (PeproTech), and 5% fetal bovine serum. The cells were plated to a density of 5×10^3 cells/cm^2 on fibronectin-coated dishes, and the medium was replaced every 2 days. For hypoxic culture, cells were cultured in a gas mixture composed of 90% N$_2$, 5% CO$_2$, and 5% O$_2$. For maintenance of the hypoxic gas mixture, a ProOx C21 carbon dioxide and oxygen controller and a C-Chamber (Biospherix) were used.

Senescence-associated β-galactosidase staining

Cells were fixed with 2% paraformaldehyde/0.2% glutaradehyde for 5 min at room temperature and then washed twice with phosphate-buffered saline (PBS). The cells were then incubated overnight at 37°C with fresh senescence-associated β-galactosidase (SA-β-Gal) chromogenic substrate solution (1 mg/mL Bluo-gal (Life Technologies), 40 mM citric acid (pH 6.0), 5 mM potassium ferrocyanide, 5 mM potassium ferricyanide, 150 mM NaCl, and 2 mM MgCl$_2$).

Measurement of ROS production

Cells were harvested and incubated with 10 μM 5-(and-6)-chloromethyl-2′,7′-dichlorodihydrofluorescein diacetate, acetyl ester (CM-H$_2$DCFDA). The amount of intracellular ROS production was proportional to the green fluorescence, as analyzed using a Guava EasyCyte 8HT flow cytometer (Millipore) using an argon laser at 488 nm and a 525/30 nm band pass filter, and dead cells were excluded using the Live/Dead Fixable Far Red Dead Cell Stain Kit (Life Technologies).

EdU proliferation assay

For assessment of cell proliferation, hADMPCs were seeded on a fibronectin-coated six-well plate at a density of 5×10^3 cells/cm^2 and cultured for 3 days. Cell proliferation was detected by incorporating of 5-ethynyl-2′-deoxyuridine (EdU) and using the Click-iT EdU Alexa Fluor 488 Flow Cytometry Assay Kit (Life Technologies). Briefly, according to the manufacturer's protocol, cells were incubated with 10 μM EdU for 2 h before fixation, permeabilized, and stained with EdU. EdU-positive cells were then analyzed using the 488 nm laser of a Guava EasyCyte 8HT flow cytometer (Millipore).

Flow cytometry analysis

Flow cytometry analysis was performed as previously described [34]. Briefly, hADMPCs were harvested and resuspended in staining buffer (PBS containing 1% BSA, 2 mM EDTA, and 0.01% sodium azide) at a density of

1×10^6 cells/mL, incubated for 20 min with a fluorescein isothiocyanate (FITC)-conjugated antibody against CD49b or CD98 (BioLegend) or a phycoerythrin (PE)-conjugated antibody against CD10, CD13, CD29, CD44, CD49a, CD49c, CD49d, CD49e, CD51/61, CD73, CD90, CD105, CD117, SSEA4, HLA-A,B,C (BioLegend), CD133/1 (Miltenyi Biotec), or CD166 (Beckman Coulter). Nonspecific staining was assessed using relevant isotype controls. Dead cells were excluded using the Live/Dead Fixable Far Red Dead Cell Stain Kit (Life Technologies). FlowJo software was used for quantitative analysis.

RNA extraction, cDNA generation, and quantitative polymerase chain reaction

Total RNA was extracted using the RNeasy Mini Kit (Qiagen) accroding to the manufacturer's instructions. cDNA was generated from 1 μg of total RNA using the Verso cDNA Synthesis Kit (Thermo Scientific) and purified using the MinElute PCR Purification Kit (Qiagen). Quantitative polymerase chain reaction (Q-PCR) analysis was conducted using the SsoFast EvaGreen supermix (Bio-Rad) according to the manufacturer's protocols. The relative expression value for each gene was calculated using the ΔΔCt method, and the most reliable internal control gene was determined using geNorm Software (http://medgen.ugent.be/~jvdesomp/genorm/). Details of the primers used in these experiments are available on request.

Western blot analysis

Whole cell extracts were prepared by washing cells with ice-cold PBS and lysing them with M-PER Mammalian Protein Extraction Reagent (Thermo Scientific Pierce) according to the manufacturer's instructions. Nuclear and cytosolic extracts were prepared as follows. Cells were washed with ice-cold PBS and lysed with lysis buffer (50 mM Tris-HCl (pH 7.5), 0.5% Triton X-100, 137.5 mM NaCl, 10% glycerol, 5 mM EDTA, 1 mM sodium vanadate, 50 mM sodium fluoride, 10 mM sodium pyrophosphate, and protease inhibitor cocktail). Then, insoluble nuclei were isolated by centrifugation and lysed with lysis buffer containing 0.5% SDS. Equal amounts of proteins were separated by sodium dodecyl sulfate polyacrylamide gel electrophoresis (SDS-PAGE), transferred to polyvinylidene fluoride membranes (Immobilon-P; Millipore), and probed with antibodies against cleaved Notch1 (#2421; Cell Signaling Technology), HIF-1α (#610959; BD Bioscience), hypoxia-inducible factor 2α (MAB3472; Millipore), Akt (#9272; Cell Signaling Technology), and phospho Akt (Ser473) (#4060; Cell Signaling Technology). Horseradish peroxidase (HRP)-conjugated anti-mouse or -rabbit IgG antibody (Cell Signaling Technology) was used as a secondary antibody, and immunoreactive bands were visualized using Immobilon Western Chemiluminescent HRP substrate (Millipore). The band intensity was measured using the ImageJ software.

Fluorescence microscopy

Phase-contrast and fluorescence images were obtained using a fluorescence microscope (BZ-9000; Keyence) using BZ Analyzer Software (Keyence).

Adipogenic, osteogenic, and chondrogenic differentiation procedures

For adipogenic differentiation, cells were cultured in differentiation medium (Zen-Bio). After 7 days, half of the medium was exchanged for adipocyte medium (Zen-Bio) and this was repeated every 3 days. Three weeks after differentiation, adipogenic differentiation was confirmed by a microscopic observation of intracellular lipid droplets with the aid of Oil Red O staining. Osteogenic differentiation was induced by culturing the cells in osteocyte differentiation medium (Zen-Bio). Differentiation was examined by Alizarin Red staining. For chondrogenic differentiation, 2×10^5 hADMSCs were centrifuged at 400 g for 10 min. The resulting pellets were cultured in chondrogenic medium (Lonza) for 21 days. The pellets were fixed with 4% paraformaldehyde in PBS, embedded in OCT, frozen, and sectioned at 8 μm. The sections were incubated with PBSMT (PBS containing 0.1% Triton X-100, and 2% skim milk) for 1 h at room temperature, and then incubated with a mouse monoclonal antibody against type II collagen (Abcam) for 1 h. After washing with PBS, cells were incubated with Alexa 546-conjugated anti-mouse IgG to identify chondrocytes (Life Technologies). The cells were counterstained with 4'-6-diamidino-2-phenylindole (DAPI) (Life Technologies) to identify cellular nuclei. The sections were also stained with 1% alcian blue (Sigma Aldrich) in 3% acetic acid, pH 2.5 for 30 min.

Determination of HK, PFK, LDH, PDH, and Cox IV activities

Cells (2×10^6) were lysed, and HK, PFK, LDH, or PDH activity was measured using the Hexokinase Colorimetric Activity Kit, Phosphofructokinase (PFK) Activity Colorimetric Assay Kit, Lactate Dehydrogenase (LDH) Activity Assay Kit, or Pyruvate Dehydrogenase Activity Colorimetric Assay Kit (all from BioVision), respectively, according to the manufacturer's instructions. To measure Cox IV activity, mitochondria were isolated from 2×10^7 cells using a Mitochondria Isolation Kit (Thermo Scientific) and lysed with buffer containing n-Dodecyl β-D-maltoside, followed by measurement with the Mitochondria Activity Assay (Cytochrome C Oxidase Activity Assay) Kit (BioChain Institute), according to the manufacturer's instructions.

Results

5% oxygen hypoxic culture condition increases proliferation capacity and decreases senescence

hADMPCs were cultured under 20% oxygen (normoxia; Nx) or 5% oxygen (hypoxia; Hx), and their proliferation capacities were examined based on the relationship between the number of cultivation days and the population doubling level (PDL). Nx-cultured hADMPCs ceased proliferation at a PDL of 35–40 (between 46–70 days), whereas continuous cell proliferation beyond 45 PDL was observed when hADMPCs were cultured in the Hx condition (Fig. 1A). To investigate whether this increase of PDL in the Hx culture condition resulted from an increase in cell cycle progression and increase in survival rates, EdU, an alternative to 5-bromo-2'-deoxyuridine (BrdU), was incorporated into the
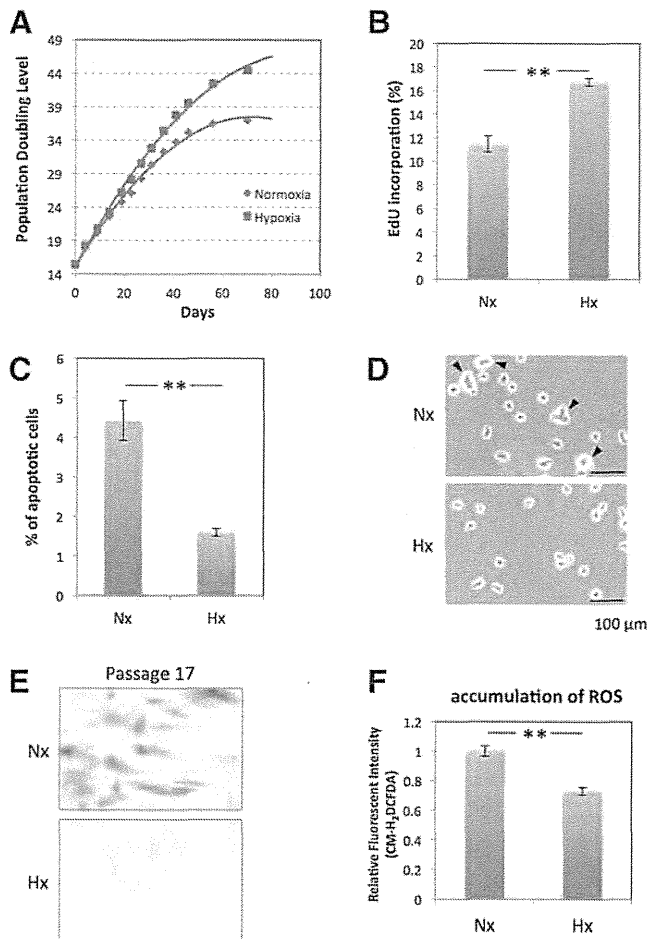
FIG. 1. Hypoxia increases proliferation capacity and decreases senescence in tissue-derived multilineage progenitor cells (hADMPCs). **(A)** Growth profiles of hADMPCs under normoxic (*red square*) and hypoxic (*blue square*) conditions. The population doubling level (PDL) was determined to be 0 when cells were isolated from human adipose tissue. Cells were maintained until they reached PDL13–15 (passage 3) and then split into four aliquots of equal cell densities. PDL was calculated based on the total cell number at each passage. **(B)** Detection of normoxic (Nx) and hypoxic (Hx) cells by flow cytometry after incorporation of EdU. **(C)** Percentages of apoptotic cells with sub-G1 DNA under Nx and Hx conditions. The results are presented as the mean of three independent experiments. **(D)** hADMPCs cultured under Nx and Hx conditions were harvested by trypsin-EDTA and then imaged using a phase-contrast microscope. *Arrowheads* indicate cells with a larger and more irregular shape. **(E)** Cells expanded under Nx and Hx conditions were stained with SA-β-gal. **(F)** Cellular reactive oxygen species detection by the oxidative stress indicator CM-H$_2$DCFDA in hADMPCs under Nx or Hx. Data are presented as the mean fluorescence intensity of three independent experiments. Error bars indicate SD. **$**P < 0.01$** indicates significant difference (independent *t*-test) between Nx and Hx. Scale bars; 100 μm. Color images available online at www.liebertpub.com/scd

genomic DNA of the hADMPCs, and the amount of incorporated EdU was quantified by flow cytometry. As shown in Fig.1B, the EdU incorporation rate was significantly higher in Hx-cultured hADMPCs than in Nx-cultured hADMPCs, suggesting that cell growth was increased in the Hx culture condition. In addition, measurement of DNA content in hADMPCs revealed a slight but significant decrease of sub-G1 peaks, which indicates the existence of apoptotic cells with degraded DNA, when the cells were cultured in the Hx condition (Fig. 1C). These data suggest that the Hx culture condition increases the proliferation capacity of hADMPCs by promoting their cell growth and survival rates. We also found that Nx-cultured hADMPCs were larger with a more irregular shape (Fig. 1D), which suggests that the Hx culture condition prevented hADMPCs from entering senescence [35]. To further investigate this phenomenon, cellular senescence was measured by staining for SA-β-Gal, which revealed that SA-β-Gal activity was increased in Nx-cultured hADMPCs at passage 17 (Fig. 1E). Since it has been hypothesized that senescence results from oxidative stress [20], accumulation of ROS in hADMPCs was detected using the nonfluorescent probe, CM-H$_2$DCFDA. Flow cytometry analysis revealed that ROS were generated at higher levels in hADMPCs when cultured in the Nx condition (Fig. 1F), suggesting that reduced production of ROS in the Hx condition may prevent the cells from entering replicative senescence.

Hypoxic culture maintains some MSC properties and increases differentiation

We then examined the cell properties of hADMPCs under Nx and Hx conditions. Initially, cell surface antigens expressed on hADMPCs were analyzed by flow cytometry. No significant difference in expression profile between hADMPCs cultured in Nx and Hx was observed; the cells were consistently positive for CD10, CD13, CD29, CD44, CD49a, CD49b, CD49c, CD49d, CD49e, CD51/61, CD54, CD59, CD73, CD90, CD98, CD105, CD166, and HLA-A, B, C, but negative for CD34, CD45, CD117, and CD133 (Fig. 2 and data not shown). These data were consistent with previous reports describing the expression profiles of cell surface markers of hMSCs [36,37]. To further examine the stem cell properties of hADMPCs, their potential for differentiation into adipocyte, osteocyte, and chondrocyte lineages was analyzed at passage 8. Hx-cultured hADMPCs presented enhanced differentiation into various lineages (Fig. 3A, B), indicating that the Hx culture condition improved the stem cell properties of hADMPCs.

Hypoxic culture condition activates Notch signaling

To reveal the molecular mechanism by which the Hx culture condition increased the proliferative capacity and maintained the stem cell properties of hADMPCs, we next examined Notch signaling, which is required for maintaining stem-cell features of various types of stem cells [30,31]. As expected, levels of cleaved NOTCH1, an activated form of NOTCH1, were significantly increased (greater than twofold) in the Hx culture condition (Fig. 4A). Q-PCR analysis revealed that HES1, a downstream target of Notch signaling, was upregulated in Hx-cultured hADMPCs, which also indicated that Notch signaling was activated in
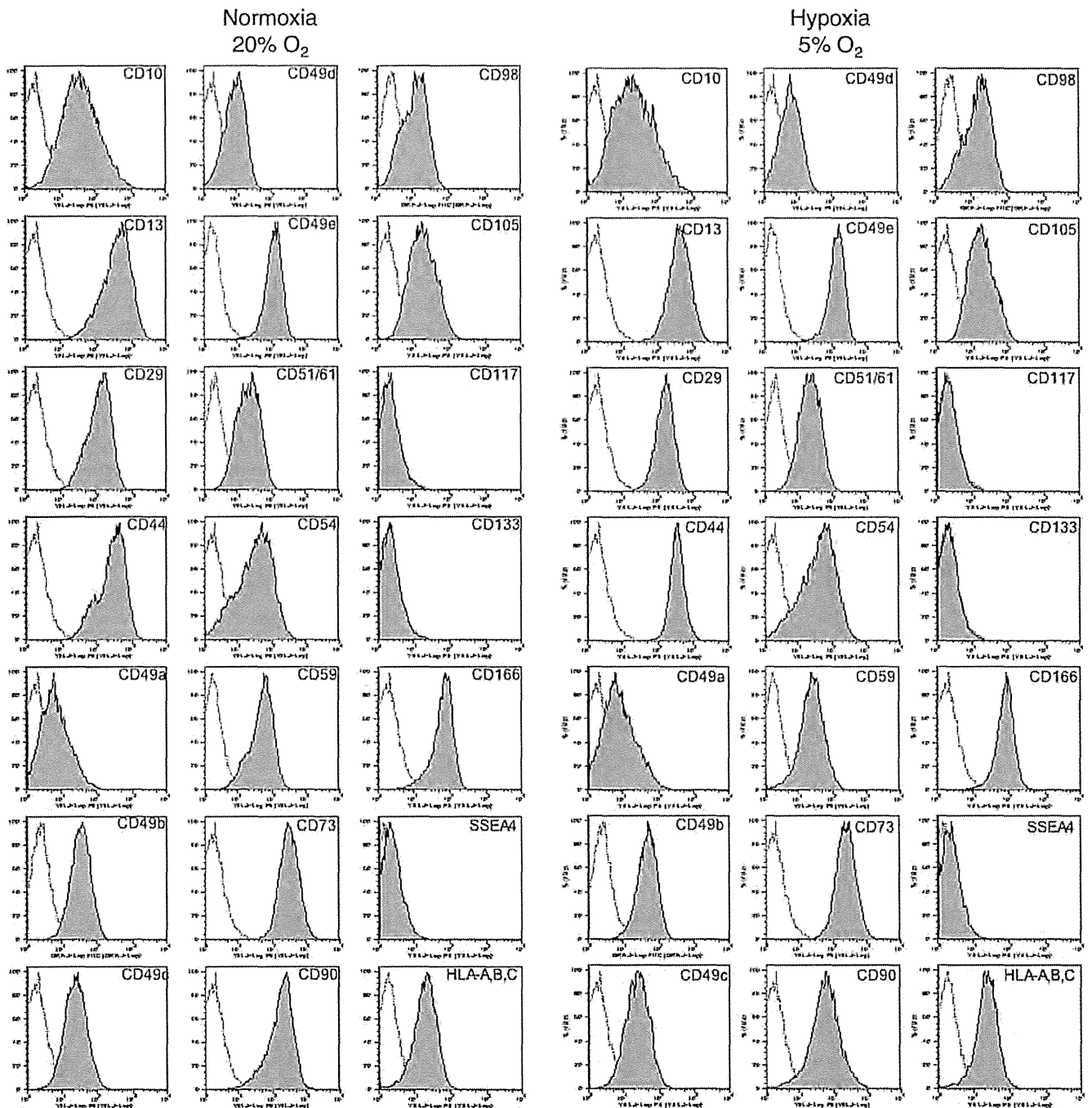
FIG. 2. Hypoxic culture maintains mesenchymal stem cell properties. hADMPCs cultured under normoxia (20% O_2) or hypoxia (5% O_2) were labeled with antibodies against the indicated antigens and analyzed by flow cytometry. Representative histograms are shown. The respective isotype control is shown as a *gray line*.

the Hx culture condition (Fig. 4B). Administration of the γ-secretase inhibitor DAPT at 1 μM, which was sufficient to inhibit the proteolytic cleavage of NOTCH1 (Fig. 4A), decreased the Hx-induced expression of HES1 at both mRNA and protein levels (Fig. 4B, C). These data indicate that Hx increased the expression of HES1 through activation of Notch signaling. It has been reported that Notch signaling and hypoxia-inducible factor (HIF) undergo crosstalk in hypoxic cells [38–41]. Therefore, HIF-1α and HIF-2α protein levels in hADMPCs were analyzed by western blotting.

HIF-1α was stabilized when a chemical hypoxia-mimicking agent, cobalt chloride, was applied in the culture; whereas no obvious increase of HIF-1α was observed in the Hx culture condition (Fig. 4D). However, we did not detect any HIF-2α expression even in the presence of cobalt chloride (Fig. 4E). Q-PCR analysis revealed that *HIF2A* mRNA was not expressed in these cells (data not shown). From these results, we concluded that neither HIF-1α nor HIF-2α was involved in the Hx-induced increase in the proliferative capacity and stem cell properties of hADMPCs.

A

B

FIG. 3. Hypoxic culture enhances stem cell properties. hADMPCs were expanded under normoxic and hypoxic conditions. (A) Normoxic (20% O₂) and hypoxic (5% O₂) cells at passage 8 were induced for 3 weeks to differentiate into osteoblasts and adipocytes and stained with Alizarin Red and Oil-Red O, respectively. The stained dye was extracted, and OD values were measured and plotted as the means of three independent experiments ± SD. *P<0.05. Scale bars, 200 μm. (B) Normoxic (20% O₂) and hypoxic (5% O₂) cells at passage 8 were induced for 3 weeks to differentiate to chondrocytes, and immunofluorescent analysis of collagen II (red) and Alucian Blue staining were performed. The blue signals indicate nuclear staining. Scale bars, 100 μm. Noninduced control cultures in growth medium without adipogenic, osteogenic or chondrogenic differentiation stimuli are shown (Undifferentiated). Color images available online at www .liebertpub.com/scd
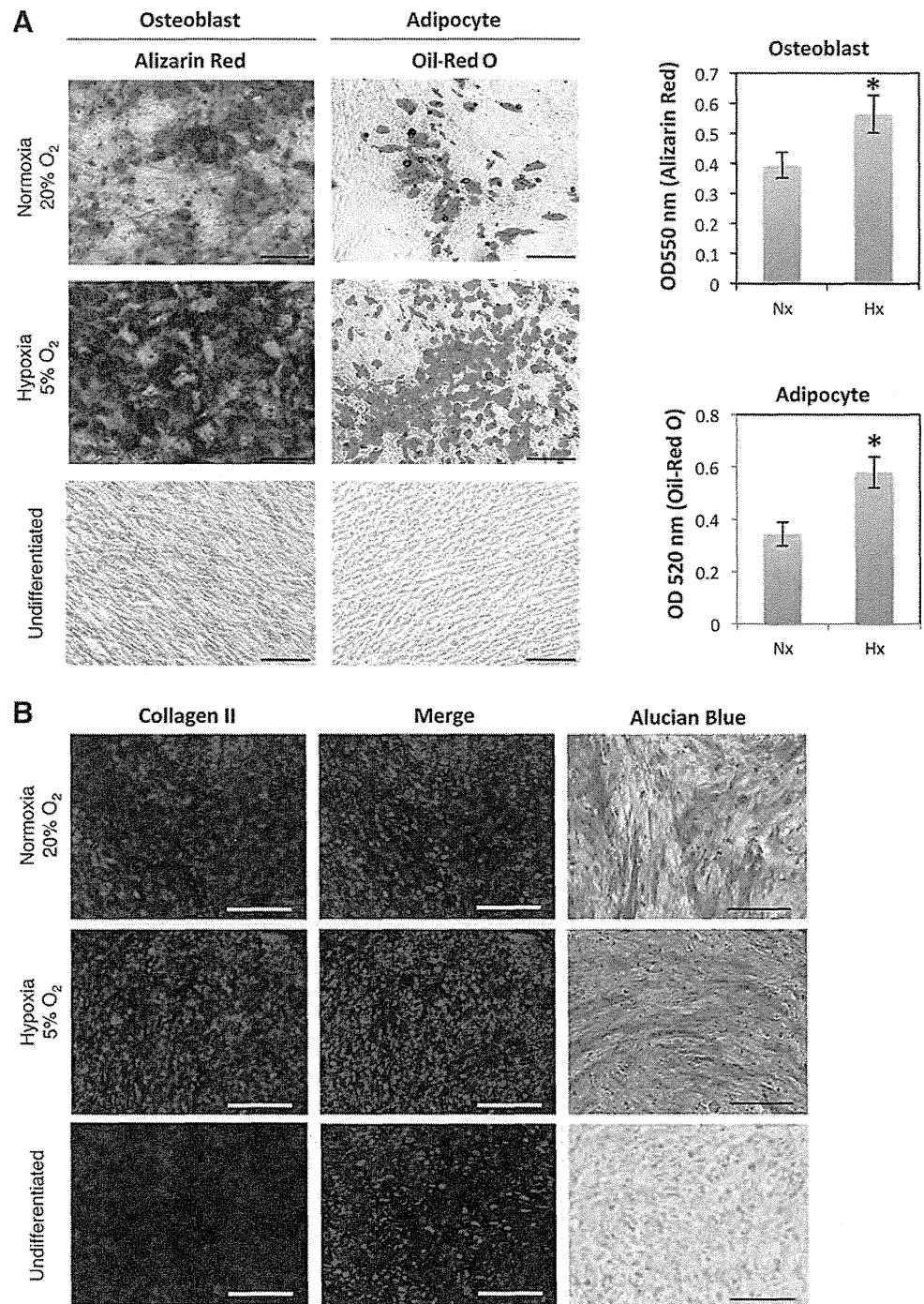
To identify the signaling responsible for the observed effect, we next examined the Akt, NF-κB, and p53 signaling pathways. It has been reported that hypoxic conditions induce the activation of Akt and NF-κB signaling [42,43]. In addition, hypoxic conditions have been shown to inhibit p53 activity [44], and crosstalk between these pathways and Notch signaling has also been demonstrated [41,45–47]. As shown in Fig. 4F, the Hx condition increased Akt phosphorylation, which was not decreased by DAPT treatment. These data demonstrate that 5% oxygen activated Akt signaling but not via Notch signaling. Similarly, the hypoxic condition induced nuclear accumulation of p65, which was

inhibited by DAPT treatment (Fig. 4G). These data suggest that NF-κB signaling is regulated by Notch signaling in hADMPCs. Furthermore, p53 was not activated under the 5% oxygen condition as assessed by detection of phospho-p53 and a p53 reporter assay. However, DAPT treatment significantly increased p53 activity (Fig. 4H, I).

Notch signaling is indispensable for acquisition of the advantageous properties of hADMPCs

We next examined the roles of Notch signaling in the proliferative capacity and stem cell properties of hADMPCs
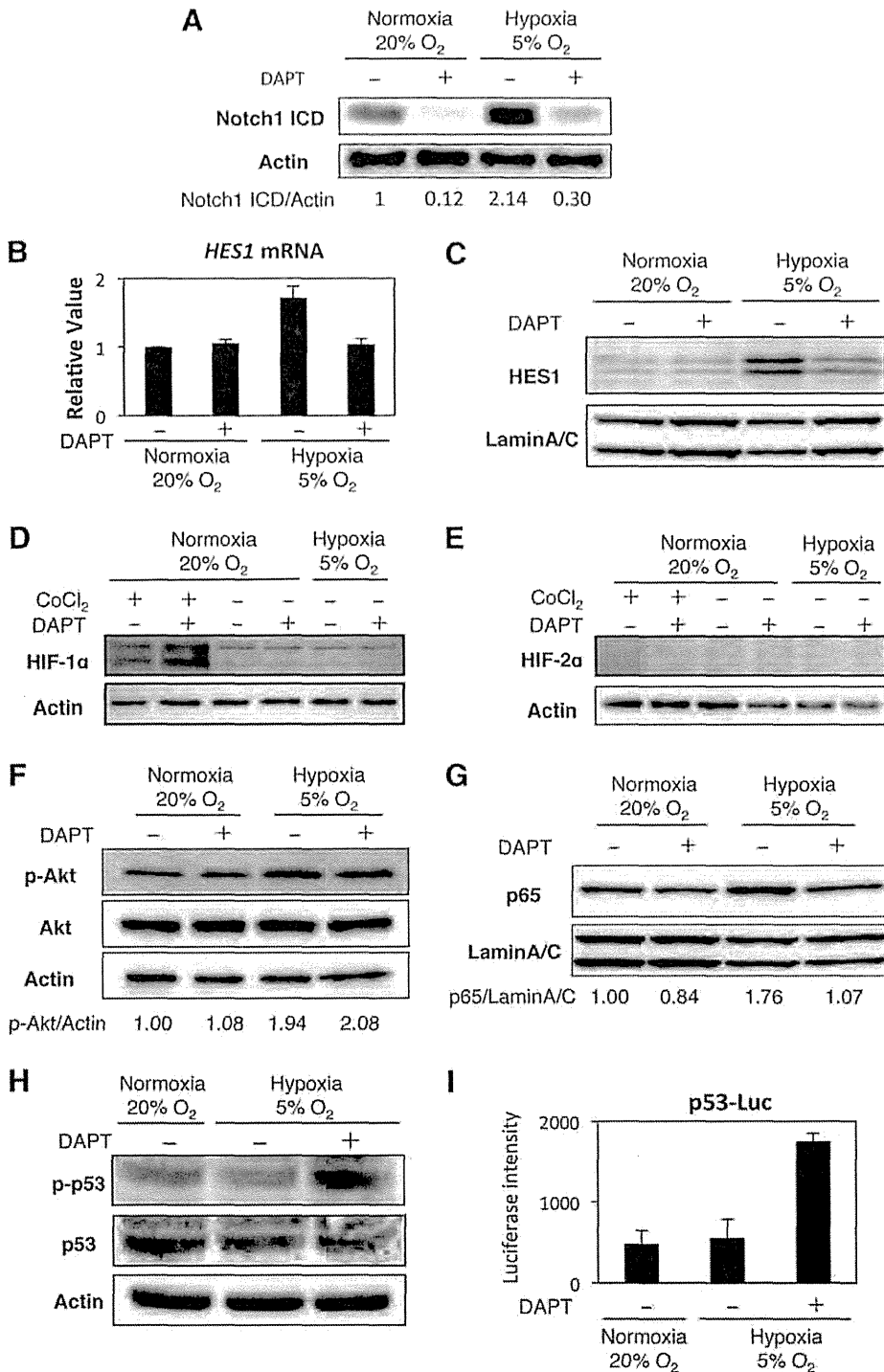
FIG. 4. Hypoxic culture condition activates Notch signaling but not HIF proteins. hADMPCs were expanded under normoxic (20% O_2) and hypoxic (5% O_2) conditions. DAPT (1 μM) was added to inhibit Notch signaling. (**A**) Western blot analysis of intracellular domain of Notch1 (Notch1 ICD) expression. Actin served as the loading control. Numbers below blots indicate relative band intensities as determined by ImageJ software. (**B**) Q-PCR analysis of *HES1*. Each expression value was calculated with the ΔΔCt method using *UBE2D2* as an internal control. (**C**) Western blot analysis of HES1 in nuclear fractions of hADMPCs. Lamin A/C served as the loading control. (**D, E**) Western blot analysis of HIF-1α (**D**) and HIF-2α (**E**). Cobalt chloride (CoCl₂) was added at a concentration of 100 μM to stabilize HIF proteins (positive control). (**F**) Western blot analysis of phosphorylated Akt (p-Akt) and Akt. Actin served as the loading control. Numbers below blots indicate relative band intensities as determined by ImageJ software. (**G**) Western blot analysis of nuclear localization of p65. Lamin A/C served as the loading control. Numbers below blots indicate relative band intensities as determined by ImageJ software. (**H**) Western blot analysis of phosphorylated p53 (p-p53) and p53. Actin served as the loading control. (**I**) Activity of p53 was measured by the p53-luciferase reporter assay. Relative luciferase activity was determined from three independent experiments and normalized to pGL4.74 activity.

in the Hx culture condition. To inhibit Notch signaling, DAPT was added to the medium at a final concentration of 1 μM. DAPT treatment significantly decreased the PDL when hADMPCs were cultured under either 20% or 5% oxygen (Fig. 5A). Intriguingly, measurement of the DNA content in hADMPCs revealed that inhibition of Notch signaling by 1 μM DAPT significantly attenuated the decrease in apoptotic cells in the Hx condition (Fig. 5B). These data suggest that 5% oxygen increases the proliferation capacity of hADMPCs through Notch signaling by

promoting their survival. To examine whether Notch signaling affects the stem cell properties of hADMPCs, differentiation into adipocyte, osteocyte, and chondrocyte lineages was analyzed at passage 8. Hx-cultured hADMPCs underwent greater differentiation into all lineages as described in Fig. 3, whereas application of a Notch inhibitor significantly decreased the differentiation capacity to all lineages (Fig. 5C–E). In addition, SA-β-Gal staining revealed that inhibition of Notch signaling by DAPT remarkably promoted senescence in both the Nx and Hx

FIG. 5. Notch signaling is indispensable for acquisition of the advantageous properties of hADMPCs. hADMPCs were expanded under normoxic (20% O₂; Nx) and hypoxic (5% O₂; Hx) conditions. DAPT (1 μM) was added to inhibit Notch signaling. **(A)** Growth profiles of hADMPCs under Nx (*red*) and Hx (*blue*) conditions. *Solid lines* represent control cells, and *dotted lines* represent DAPT-treated cells. The number of population doublings was calculated based on the total cell number at each passage. **(B)** Percentages of apoptotic cells with sub-G1 DNA. Results are presented as the mean of three independent experiments ± SD. **(C, D)** hADMPCs at passage 8 were induced for 3 weeks to differentiate into adipocytes **(C)** and osteoblasts **(D)** and stained with Oil Red O and Alizarin Red, respectively. The stained dye was extracted, and OD values were measured and plotted as the means of three independent experiments ± SD. **(E)** hADMPCs at passage 8 were induced for 3 weeks to differentiate into chondrocytes, and an immunofluorescent analysis of collagen II (*red*) was performed. The *blue* signals indicate nuclear staining. **(F)** hADMPCs were stained with SA-β-gal. *P < 0.05 and **P < 0.01 indicate significant differences (independent *t*-test) between Nx and Hx. Scale bars; 100 μm. Color images available online at www.liebertpub.com/scd
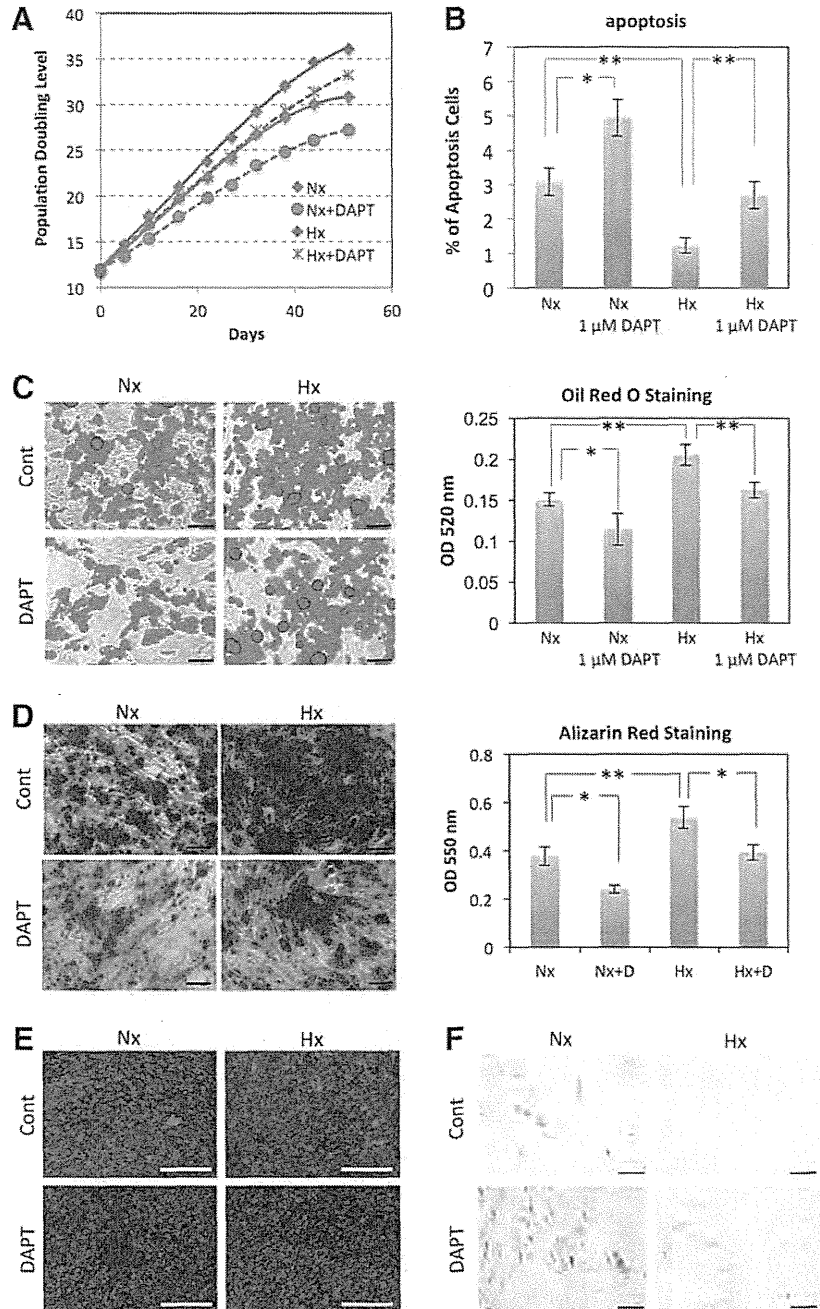
culture conditions, suggesting that the suppression of replicative senescence observed in the Hx condition is mediated by Notch signaling (Fig. 5F).

Glycolysis is enhanced in the 5% oxygen condition through Notch signaling

Recent studies suggest that the metabolic shift from aerobic mitochondrial respiration to glycolysis extends the life span possibly via reduction of intrinsic ROS production [18,19]. Our results demonstrate that the 5% oxygen condition reduced ROS accumulation in hADMPCs (Fig. 1F). In addition, the relationship between Notch signaling and glycolysis has been recently established [48,49]. We, therefore, considered glycolytic flux by measuring the glu-

cose consumption and lactate production of hADMPCs in the Nx or Hx culture conditions. As shown in Fig. 6A, glucose consumption and lactate production were elevated in the Hx culture condition, indicating that a metabolic shift to glycolysis occurred when hADMPCs were cultured in 5% oxygen. In contrast, the Notch inhibitor DAPT markedly reduced glycolytic flux as assessed by glucose consumption and lactate production (Fig. 6A). To identify the genes responsible for the glycolytic change, we performed a Q-PCR analysis. As shown in Fig. 6B, *SLC2A3, TPI, and PGK1*, encoding glycolytic enzymes, were upregulated in the 5% oxygen condition; whereas these genes were suppressed by DAPT treatment. Interestingly, Hes1 transduction by an adenoviral vector markedly induced the mRNA expression of the same genes (Fig. 6E). In addition, SCO2, a positive
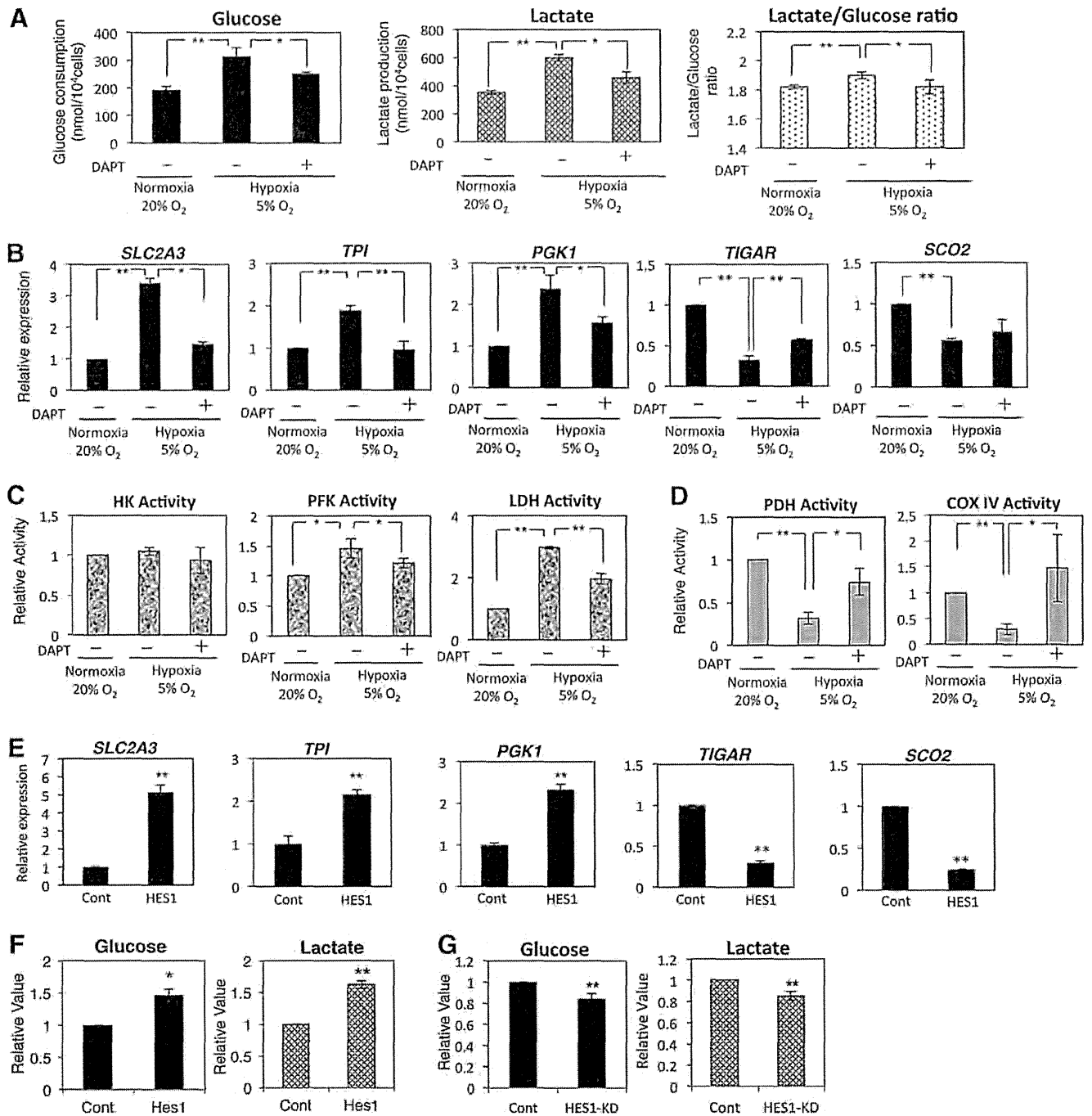
FIG. 6. Glycolysis is enhanced under 5% oxygen through Notch signaling. (A–D) hADMPCs were expanded under normoxic (20% O₂) and hypoxic (5% O₂) conditions. DAPT (1 μM) was added to inhibit Notch signaling. (A) Glucose consumption and lactate production of hADMPCs were measured and plotted as the means of three independent experiments ± SD. (B) Relative mRNA expression of *SLC2A3*, *TPI*, *PGK1*, *TIGAR*, and *SCO2* in hADMPCs. Each expression value was calculated with the ΔΔCt method using *UBE2D2* as an internal control. (C, D) Hexokinase (HK), phospho-fructokinase (PFK), lactate dehydrogenase (LDH) (C), pyruvate dehydrogenase (PDH), and Complex IV (Cox IV) (D) activities were measured and the value of relative activity was plotted as the means of three independent experiments ± SD. (E, F) hADMPCs were transduced with either mock (Cont) or HES1 and then cultured for 3 days. (E) Relative mRNA expression of *SLC2A3*, *TPI*, *PGK1*, *TIGAR*, and *SCO2* in hADMPCs. Each expression value was calculated with the ΔΔCt method using *UBE2D2* as an internal control. (F) Glucose consumption and lactate production of hADMPCs were measured and plotted as the means of three independent experiments ± SD. (G) hADMPCs were transduced with either scrambled control RNAi (Cont) or RNAi against HES1 (HES1-KD), and then cultured for 3 days. Glucose consumption and lactate production of hADMPCs were measured and plotted as the means of three independent experiments ± SD. **$P < 0.01$. *$0.01 < P < 0.05$.
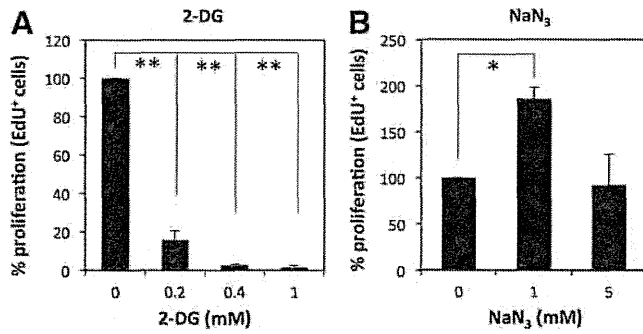
FIG. 7. Glycolysis supports proliferation of hADMPCs. hADMPCs were treated with 0, 0.2, 0.4, and 1 mM 2-deoxy-D-glucose (2-DG) **(A)** or 0, 1, and 5 mM sodium azide (NaN₃) **(B)** for 24 h. Cells were then allowed to incorporate EdU for 2 h, and the EdU-positive cells were analyzed by flow cytometry. The percentages for the 0 mM control were plotted as the means of three independent experiments ± SD. $*P < 0.05$; $**P < 0.01$.

modulator of aerobic respiration, and TIGAR, a negative regulator of glycolysis, were transcriptionally downregulated in the 5% oxygen condition; whereas DAPT treatment partially restored the expression level (Fig. 6B). Adenoviral expression of Hes1 dramatically reduced *SCO2* and *TIGAR* expression (Fig. 6E), which suggests that the Notch-Hes1 signaling modulates the metabolic pathway. We also measured the activities of key enzymes in glycolysis. Hexokinase activity was not changed under hypoxic conditions; however, PFK and LDH were activated in 5% oxygen condition, which was attenuated by Notch inhibition (Fig. 6C). In addition, pyruvate dehydrogenase (PDH) and cytochrome c oxidase (Complex IV) activity assays showed that mitochondrial respiration decreased under the hypoxic condition and that DAPT treatment restored it (Fig. 6D). Moreover, glycolytic flux in Hes1-expressing hADMPCs was positively correlated with the expression of these glycolytic genes as assessed by glucose consumption and lactate production (Fig. 6F). In contrast, HES1 knockdown by adenoviral transduction of *HES1* RNAi resulted in a significant reduction of glycolytic flux (Fig. 6G), demonstrating that HES1 is involved in the regulation of glycolysis.

Glycolysis supports the proliferation of hADMPCs

To determine whether aerobic glycolysis is important for the proliferation of hADMPCs, hADMPCs were treated with the glycolytic inhibitor 2-deoxy-D-glucose (2-DG) or the respiration inhibitor sodium azide (NaN₃). We found that hADMPCs were sensitive to treatment with 2-DG even at a low concentration of 0.2 mM (Fig. 7A). In contrast, treatment of hADMPCs with NaN₃ rather increased their proliferation at the concentration of 1 mM and supported their proliferation even at the concentration of 5 mM (Fig. 7B). These data suggest that the proliferation of hADMPCs is compromised when aerobic glycolysis is blocked.

Discussion

Recent evidence suggests that hypoxic culture conditions confer a growth advantage, prevent premature senescence, and maintain undifferentiated states in ESCs, iPSCs, and

somatic stem cells. However, the molecular mechanism underlying the beneficial effects of culturing these cells at low oxygen conditions remains unclear. Our findings prompted us to hypothesize that Notch signaling in physiological hypoxic conditions (5% O₂) contributes to these effects on hADMPCs by modulating glycolytic flux.

We found that 5% O₂ significantly increased the proliferation capacity, decreased apoptosis, and inhibited senescence of hADMPCs (Fig. 1). Moreover, 5% O₂ improved the differentiation of hADMPCs without affecting the expression of their cell surface markers (Figs. 2 and 3). Welford et al. reported that HIF-1α delays premature senescence of mouse embryonic fibroblasts under hypoxic conditions (2% O₂) [50]. Tsai et al. reported that hypoxia (1% O₂) inhibits senescence and maintains MSC properties through accumulation of HIF-1α [26]. Hypoxia was recently reported to enhance the undifferentiated status and stem cell properties in various stem and precursor cell populations via the interaction of HIF with the Notch intracellular domain to activate Notch-responsive promoters [38]. In the current study, the effects observed in 5% O₂ condition were independent of HIF proteins, because accumulation of HIF-1α and HIF-2α was not observed (Fig. 4). Instead, our findings suggest that 5% O₂ activated Notch signaling, which contributed advantageous effects of hypoxic culture on hADMPCs. A pharmacological inhibitor of Notch signaling, DAPT, abrogated the hypoxic-induced Notch activation, increased proliferation capacity and lifespan, maintenance of stem cell properties, and prevention of senescence (Figs. 4 and 5). Moreover, we also found that 5% O₂ enhanced glucose consumption and lactate production, and these effects were also attenuated by Notch inhibition (Fig. 6A) and knockdown of HES1 (Fig. 6G). Previously, it has been reported that Notch signaling promotes glycolysis by activating the PI(3)K-Akt pathway [48,49]. However, our results indicate that Akt signaling was not activated by Notch signaling, because DAPT did not attenuate hypoxia-induced Akt phosphorylation (Fig. 4F). Although Akt is unlikely to be regulated by Notch signaling in hADMPCs, it is obvious in our data that Akt signaling was activated by 5% O₂. Therefore, we could not rule out the possibility that the promotion of glycolysis in the 5% O₂ condition was caused by Akt signaling.

Recent evidence suggests that Notch signaling acts as a metabolic switch [48,51]. Zhou et al. demonstrated that hairy, a basic helix-loop-helix transcriptional repressor regulated by Notch signaling, was upregulated and genes encoding metabolic enzymes, including TCA cycle enzymes and respiratory chain complexes, were downregulated in hypoxia-tolerant flies. Intriguingly, they also found that hairy-binding elements were present in the regulatory region of the downregulated metabolic genes. Their work, thus, provides new evidence that hairy acts as a metabolic switch [51]. Landor et al. demonstrated that both hyper- and hypoactive Notch signaling induced glycolysis, albeit by different mechanisms. They showed that Notch activation increased glycolysis through activation of PI3K-AKT signaling, whereas decreased Notch activity inhibited mitochondrial function in a p53-dependent manner in MCF7 breast cancer cell lines [48]. Consistent with their reports, our findings that Notch signaling promoted activity of some glycolysis enzymes and inhibited mitochondrial activity

(Fig. 6) also suggest that Notch signaling functioned as a metabolic switch. While our data showed that Notch inhibition by DAPT resulted in reduced glycolysis (Fig. 6A–C), induction of mitochondrial function (Fig. 6D) and activation of p53 (Fig. 4H, I) are not consistent with the report of Landor el al. This contradiction might be explained by the expression level of endogenous Notch. Landor et al. showed that in breast cancer MDA-M-231 cells, which showed higher endogenous Notch activity, high glucose uptake, and lactate production than MCF7 breast cancer cell lines, Notch inhibition by DAPT significantly reduced glucose consumption and lactate production [48]. As shown in Fig. 4A, we observed that hADMPCs in 5% O_2 displayed high Notch activity. Moreover, the lactate-to-glucose ratio was 1.8–1.9 in hADMPCs, suggesting that hADMPCs largely rely on glycolysis for energy production (Fig. 6A). In addition, it was reported that hMSCs showed a higher glycolytic rate than primary human fibroblast [52]. It appears that hADMPCs cultured under hypoxic conditions might possess cell properties similar to MDA-M-231 cells or MCF7 cells, in which stable expression of constructs NICD1-GFP produces high Notch activity.

Nuclear translocation of p65 was observed in hypoxic conditions, demonstrating that NF-κB is a direct target of Notch signaling (Fig. 4G). Intriguingly, the hypoxic culture conditions in this study upregulated several genes encoding glycolytic enzymes (SLC2A3, TPI, and PGK1); whereas the expression of these genes was suppressed by Notch inhibition. In addition, Hes1 transduction induced mRNA expression of the same genes (Fig. 6). It was previously reported that SLC2A3 expression was regulated by p65/NF-κB signaling, and that Notch/Hes1 is able to induce the activation of the NF-κB pathway in human T-ALL lines and animal disease models [53]. Espinosa et al. demonstrated that Hes1 directly targeted the deubiquitinase CYLD, resulting in deubiquitination and inactivation of TAK1 and IKK, degradation of IκBa, and activation of NF-κB signaling [53]. In our systems, however, we did not observe repression of CYLD mRNA in Hes1-overexpressing hADMPCs (data not shown). While PGK1 mRNA has been reported to be upregulated by NF-κB, it has not clearly been shown to be controlled by NF-κB despite the presence of an NF-κB site in the promoter [54]. Although modulation of TPI expression by NF-κB has not been reported, we found several NF-κB binding sites on the human TPI promoter (data not shown). Since NF-κB is likely to be one of the responsible signals for hypoxic-induced glycolysis [53], further analysis will be required to determine the mechanism by which NF-κB signaling is induced by Notch signaling. In addition, it will be important to investigate whether NF-κB is really responsible for the observed glycolysis and whether it regulates the expression of SLC2A3, TPI, and PGK1 in hADMPCs under 5% oxygen.

In addition, SCO2, a positive modulator of aerobic respiration, and TIGAR, a negative regulator of glycolysis, were transcriptionally downregulated in the 5% oxygen condition; whereas DAPT treatment partially restored expression (Fig. 6B). We observed some glycolysis and mitochondrial enzyme activity and found that the activities of COX IV and PFK were consistent with gene expression data (Fig. 6C, D). Adenoviral expression of Hes1 dramatically reduced SCO2 and TIGAR expression (Fig. 6E), which

suggests that Notch-Hes1 signaling modulates the metabolic pathway. Intriguingly, our results also indicate that Hes1 could suppress the expression of TIGAR and SCO2, a p53 target gene. It has been reported that Notch signaling suppresses p53 in lymphomagenesis [46]. Moreover, Kim et al. reported that NICD1 inhibits p53 phosphorylation and represses p53 transactivation by interacting with p53 [47]. In addition, DAPT treatment resulted in the enhancement of p53 activity in the hypoxic conditions (Fig. 4H, I). Therefore, it is possible that p53 activation was regulated by Notch signaling in hADMPCs, although we did not observe a decrease in p53 activity in hypoxic conditions in this study (Fig. 4). Further analysis will be required to determine whether p53 activity is suppressed in hypoxic conditions over a longer period of culture.

Cells undergoing active proliferation utilize large amounts of glucose through glycolysis, producing pyruvate for use in substrates (amino acids and lipids) and the pentose shunt for use in nucleic acid substrates, and also producing NADPH as a reducing agent to counter oxidative stress [18,55]. In the current study, 5% O_2 actually increased proliferation and decreased the accumulation of ROS, which may be involved in the reduction of senescence (Fig. 1). Since accumulation of endogenous ROS might be a major reason for replicative senescence [20], enhancing glycolysis in cultured cells may improve the quality of the cells by suppressing premature senescence. Kondoh et al. demonstrated that enhanced glycolysis is involved in cellular immortalization through reduction of intrinsic ROS production [14,18,19]. Therefore, it is possible that the extension of lifespan observed in our experimental conditions was caused by the reduction of intracellular ROS levels through enhanced glycolysis by Notch signaling. Our data indicate that aerobic glycolysis is utilized for proliferation of hADMPCs, because the glycolytic inhibitor 2-DG attenuates the proliferation rate of hADMPCs (Fig. 7A). Intriguingly, the aerobic respiration block by NaN3 did not decrease the proliferation; rather, it increased proliferation at a low concentration (Fig. 7B), which may support our data indicating that the metabolic switch from mitochondrial respiration to glycolysis provides a growth advantage to hADMPCs. However, the question of whether the enhanced glycolysis really contributes to the prolonged lifespan in hADMPCs remains to be determined in this study.

In the current study, the molecular mechanism for how Notch signaling is activated in 5% O_2 conditions was explored. It has been reported that Notch1 activity is influenced by oxygen concentration [40,41,56]. In melanoma cells, hypoxia (2% O_2) resulted in increased expression of Notch1 by HIF-1α and also by Akt through NF-κB activity [41]. Similarly, in hypoxic breast cancer cells, Notch ligand JAG2 was shown to be transcriptionally activated by hypoxia (1% O_2) in an HIF-1α-dependent manner, resulting in an elevation of Notch signaling [40]. In contrast, in hESCs continuously cultured in 5% O_2, alteration of the Notch pathway seems to be independent of HIF-1α [56]. In our system, Notch1 activation was not likely dependent on HIF-1α and HIF-2α, because these proteins did not accumulate in the Hx condition. In contrast, our results indicate that the 5% O_2 condition activated Akt and NF-κB signaling (Fig. 4), which suggests that these molecules may activate Notch signaling in hADMPCs. NF-κB was previously shown to

increase Notch1 activity indirectly by increasing the expression of Notch ligand Jagged1 in HeLa, lymphoma, and myeloma cells [57]. In addition, Akt regulated Notch1 by increasing Notch1 transcription through the activity of NF-κB in melanoma cells [41]. Further analysis is required to clarify the mechanism underlying this phenomenon.

In conclusion, the 5% oxygen condition conferred a growth advantage through a metabolic shift to glycolysis, improved the proliferation efficiency, prevented the cellular senescence, and maintained the undifferentiated status of hADMPCs. These observations, thus, provide new regulatory mechanisms for the maintenance of stemness observed in 5% oxygen conditions. In addition, our study sheds new light on the regulation of replicative senescence, which might have an impact for quality control of hADMPC preparations used for therapeutic applications.

Acknowledgments

Author Disclosure Statement

The authors declare no conflict of interest. No competing financial interests exist.

References

1. Okura H, H Komoda, A Saga, A Kakuta-Yamamoto, Y Hamada, Y Fumimoto, CM Lee, A Ichinose, Y Sawa and A Matsuyama. (2010). Properties of hepatocyte-like cell clusters from human adipose tissue-derived mesenchymal stem cells. Tissue Eng Part C Methods 16:761–770.
2. Okura H, A Matsuyama, CM Lee, A Saga, A Kakuta-Yamamoto, A Nagao, N Sougawa, N Sekiya, K Takekita, et al. (2010). Cardiomyoblast-like cells differentiated from human adipose tissue-derived mesenchymal stem cells improve left ventricular dysfunction and survival in a rat myocardial infarction model. Tissue Eng Part C Methods 16:417–425.
3. Okura H, H Komoda, Y Fumimoto, CM Lee, T Nishida, Y Sawa and A Matsuyama. (2009). Transdifferentiation of human adipose tissue-derived stromal cells into insulin-producing clusters. J Artif Organs 12:123–130.
4. Safford KM, SD Safford, JM Gimble, AK Shetty and HE Rice. (2004). Characterization of neuronal/glial differentiation of murine adipose-derived adult stromal cells. Exp Neurol 187:319–328.
5. Leu S, YC Lin, CM Yuen, CH Yen, YH Kao, CK Sun and HK Yip. (2010). Adipose-derived mesenchymal stem cells markedly attenuate brain infarct size and improve neurological function in rats. J Transl Med 8:63.
6. Ikegame Y, K Yamashita, S Hayashi, H Mizuno, M Tawada, F You, K Yamada, Y Tanaka, Y Egashira, et al. (2011). Comparison of mesenchymal stem cells from adipose tissue and bone marrow for ischemic stroke therapy. Cytotherapy 13:675–685.
7. Tan B, Z Luan, X Wei, Y He, G Wei, BH Johnstone, M Farlow and Y Du. (2011). AMP-activated kinase mediates adipose stem cell-stimulated neuritogenesis of PC12 cells. Neuroscience 181:40–47.
8. Reid AJ, M Sun, M Wiberg, S Downes, G Terenghi and PJ Kingham. (2011). Nerve repair with adipose-derived stem cells protects dorsal root ganglia neurons from apoptosis. Neuroscience 199:515–522.
9. Rehman J, D Traktuev, J Li, S Merfeld-Clauss, CJ Temm-Grove, JE Bovenkerk, CL Pell, BH Johnstone, RV Considine and KL March. (2004). Secretion of angiogenic and antiapoptotic factors by human adipose stromal cells. Circulation 109:1292–1298.
10. Lee EY, Y Xia, WS Kim, MH Kim, TH Kim, KJ Kim, BS Park and JH Sung. (2009). Hypoxia-enhanced wound-healing function of adipose-derived stem cells: increase in stem cell proliferation and up-regulation of VEGF and bFGF. Wound Repair Regen 17:540–547.
11. Moriyama M, H Moriyama, A Ueda, Y Nishibata, H Okura, A Ichinose, A Matsuyama and T Hayakawa. (2012). Human adipose tissue-derived multilineage progenitor cells exposed to oxidative stress induce neurite outgrowth in PC12 cells through p38 MAPK signaling. BMC Cell Biol 13:21.
12. Wu H, Z Ye and RI Mahato. (2011). Genetically modified mesenchymal stem cells for improved islet transplantation. Mol Pharm 8:1458–1470.
13. Wagner W, P Horn, M Castoldi, A Diehlmann, S Bork, R Saffrich, V Benes, J Blake, S Pfister, V Eckstein and AD Ho. (2008). Replicative senescence of mesenchymal stem cells: a continuous and organized process. PLoS One 3: e2213.
14. Kondoh H, ME Lleonart, Y Nakashima, M Yokode, M Tanaka, D Bernard, J Gil and D Beach. (2007). A high glycolytic flux supports the proliferative potential of murine embryonic stem cells. Antioxid Redox Signal 9:293–299.
15. Prigione A, B Fauler, R Lurz, H Lehrach and J Adjaye. (2010). The senescence-related mitochondrial/oxidative stress pathway is repressed in human induced pluripotent stem cells. Stem Cells 28:721–733.
16. Varum S, AS Rodrigues, MB Moura, O Momcilovic, C At Easley, J Ramalho-Santos, B Van Houten and G Schatten. (2011). Energy metabolism in human pluripotent stem cells and their differentiated counterparts. PLoS One 6:e20914.
17. Warburg O, F Wind and E Negelein. (1927). The Metabolism of tumors in the body. J Gen Physiol 8:519–530.
18. Kondoh H. (2008). Cellular life span and the Warburg effect. Exp Cell Res 314:1923–1928.
19. Kondoh H, ME Lleonart, J Gil, J Wang, P Degan, G Peters, D Martinez, A Carnero and D Beach. (2005). Glycolytic enzymes can modulate cellular life span. Cancer Res 65: 177–185.
20. Beckman KB and BN Ames. (1998). The free radical theory of aging matures. Physiol Rev 78:547–581.
21. Ezashi T, P Das and RM Roberts. (2005). Low O2 tensions and the prevention of differentiation of hES cells. Proc Natl Acad Sci U S A 102:4783–4788.
22. Forristal CE, KL Wright, NA Hanley, RO Oreffo and FD Houghton. (2010). Hypoxia inducible factors regulate pluripotency and proliferation in human embryonic stem cells cultured at reduced oxygen tensions. Reproduction 139:85–97.
23. Yoshida Y, K Takahashi, K Okita, T Ichisaka and S Yamanaka. (2009). Hypoxia enhances the generation of induced pluripotent stem cells. Cell Stem Cell 5:237–241.

24. Takubo K, N Goda, W Yamada, H Iriuchishima, E Ikeda, Y Kubota, H Shima, RS Johnson, A Hirao, M Suematsu and T Suda. (2010). Regulation of the HIF-1alpha level is essential for hematopoietic stem cells. Cell Stem Cell 7:391–402.

25. Santilli G, G Lamorte, L Carlessi, D Ferrari, L Rota Nodari, E Binda, D Delia, AL Vescovi and L De Filippis. (2010). Mild hypoxia enhances proliferation and multipotency of human neural stem cells. PLoS One 5:e8575.

26. Tsai CC, YJ Chen, TL Yew, LL Chen, JY Wang, CH Chiu and SC Hung. (2011). Hypoxia inhibits senescence and maintains mesenchymal stem cell properties through down-regulation of E2A-p21 by HIF-TWIST. Blood 117:459–469.

27. Takubo K, G Nagamatsu, CI Kobayashi, A Nakamura-Ishizu, H Kobayashi, E Ikeda, N Goda, Y Rahimi, RS Johnson, et al. (2013). Regulation of glycolysis by pdk functions as a metabolic checkpoint for cell cycle quiescence in hematopoietic stem cells. Cell Stem Cell 12:49–61.

28. Grayson WL, F Zhao, R Izadpanah, B Bunnell and T Ma. (2006). Effects of hypoxia on human mesenchymal stem cell expansion and plasticity in 3D constructs. J Cell Physiol 207:331–339.

29. Wang DW, B Fermor, JM Gimble, HA Awad and F Guilak. (2005). Influence of oxygen on the proliferation and metabolism of adipose derived adult stem cells. J Cell Physiol 204:184–191.

30. Moriyama M, M Osawa, SS Mak, T Ohtsuka, N Yamamoto, H Han, V Delmas, R Kageyama, F Beermann, L Larue and S Nishikawa. (2006). Notch signaling via Hes1 transcription factor maintains survival of melanoblasts and melanocyte stem cells. J Cell Biol 173:333–339.

31. Chiba S. (2006). Notch signaling in stem cell systems. Stem Cells 24:2437–2447.

32. Okura H, A Saga, Y Fumimoto, M Soeda, M Moriyama, H Moriyama, K Nagai, CM Lee, S Yamashita, et al. (2011). Transplantation of human adipose tissue-derived multi-lineage progenitor cells reduces serum cholesterol in hyperlipidemic Watanabe rabbits. Tissue Eng Part C Methods 17:145–154.

33. Saga A, H Okura, M Soeda, J Tani, Y Fumimoto, H Komoda, M Moriyama, H Moriyama, S Yamashita, et al. (2011). HMG-CoA reductase inhibitor augments the serum total cholesterol-lowering effect of human adipose tissue-derived multilineage progenitor cells in hyperlipidemic homozygous Watanabe rabbits. Biochem Biophys Res Commun 412:50–54.

34. Moriyama H, M Moriyama, K Sawaragi, H Okura, A Ichinose, A Matsuyama and T Hayakawa. (2013). Tightly regulated and homogeneous transgene expression in human adipose-derived mesenchymal stem cells by lentivirus with tet-off system. PLoS One 8:e66274.

35. Sekiya I, BL Larson, JR Smith, R Pochampally, JG Cui and DJ Prockop. (2002). Expansion of human adult stem cells from bone marrow stroma: conditions that maximize the yields of early progenitors and evaluate their quality. Stem Cells 20:530–541.

36. Wagner W, F Wein, A Seckinger, M Frankhauser, U Wirkner, U Krause, J Blake, C Schwager, V Eckstein, W Ansorge and AD Ho. (2005). Comparative characteristics of mesenchymal stem cells from human bone marrow, adipose tissue, and umbilical cord blood. Exp Hematol 33:1402–1416.

37. Hass R, C Kasper, S Bohm and R Jacobs. (2011). Different populations and sources of human mesenchymal stem cells (MSC): A comparison of adult and neonatal tissue-derived MSC. Cell Commun Signal 9:12.

38. Gustafsson MV, X Zheng, T Pereira, K Gradin, S Jin, J Lundkvist, JL Ruas, L Poellinger, U Lendahl and M Bondesson. (2005). Hypoxia requires notch signaling to maintain the undifferentiated cell state. Dev Cell 9:617–628.

39. Zheng X, S Linke, JM Dias, X Zheng, K Gradin, TP Wallis, BR Hamilton, M Gustafsson, JL Ruas, et al. (2008). Interaction with factor inhibiting HIF-1 defines an additional mode of cross-coupling between the Notch and hypoxia signaling pathways. Proc Natl Acad Sci U S A 105:3368–3373.

40. Pietras A, K von Stedingk, D Lindgren, S Pahlman and H Axelson. (2011). JAG2 induction in hypoxic tumor cells alters Notch signaling and enhances endothelial cell tube formation. Mol Cancer Res 9:626–636.

41. Bedogni B, JA Warneke, BJ Nickoloff, AJ Giaccia and MB Powell. (2008). Notch1 is an effector of Akt and hypoxia in melanoma development. J Clin Invest 118:3660–3670.

42. Beitner-Johnson D, RT Rust, TC Hsieh and DE Millhorn. (2001). Hypoxia activates Akt and induces phosphorylation of GSK-3 in PC12 cells. Cell Signal 13:23–27.

43. Culver C, A Sundqvist, S Mudie, A Melvin, D Xirodimas and S Rocha. (2010). Mechanism of hypoxia-induced NF-kappaB. Mol Cell Biol 30:4901–4921.

44. Rohwer N, C Dame, A Haugstetter, B Wiedenmann, K Detjen, CA Schmitt and T Cramer. (2010). Hypoxia-inducible factor 1alpha determines gastric cancer chemosensitivity via modulation of p53 and NF-kappaB. PLoS One 5:e12038.

45. Espinosa L, S Cathelin, T D'Altri, T Trimarchi, A Statnikov, J Guiu, V Rodilla, J Ingles-Esteve, J Nomdedeu, et al. (2010). The Notch/Hes1 pathway sustains NF-kappaB activation through CYLD repression in T cell leukemia. Cancer Cell 18:268–281.

46. Beverly LJ, DW Felsher and AJ Capobianco. (2005). Suppression of p53 by Notch in lymphomagenesis: implications for initiation and regression. Cancer Res 65:7159–7168.

47. Kim SB, GW Chae, J Lee, J Park, H Tak, JH Chung, TG Park, JK Ahn and CO Joe. (2007). Activated Notch1 interacts with p53 to inhibit its phosphorylation and transactivation. Cell Death Differ 14:982–991.

48. Landor SK, AP Mutvei, V Mamaeva, S Jin, M Busk, R Borra, TJ Gronroos, P Kronqvist, U Lendahl and CM Sahlgren. (2011). Hypo- and hyperactivated Notch signaling induce a glycolytic switch through distinct mechanisms. Proc Natl Acad Sci U S A 108:18814–18819.

49. Ciofani M and JC Zuniga-Pflucker. (2005). Notch promotes survival of pre-T cells at the beta-selection checkpoint by regulating cellular metabolism. Nat Immunol 6:881–888.

50. Welford SM, B Bedogni, K Gradin, L Poellinger, M Broome Powell and AJ Giaccia. (2006). HIF1alpha delays premature senescence through the activation of MIF. Genes Dev 20:3366–3371.

51. Zhou D, J Xue, JC Lai, NJ Schork, KP White and GG Haddad. (2008). Mechanisms underlying hypoxia tolerance in Drosophila melanogaster: hairy as a metabolic switch. PLoS Genet 4:e1000221.

52. Funes JM, M Quintero, S Henderson, D Martinez, U Qureshi, C Westwood, MO Clements, D Bourboulia, RB Pedley,

S Moncada and C Boshoff. (2007). Transformation of human mesenchymal stem cells increases their dependency on oxidative phosphorylation for energy production. Proc Natl Acad Sci U S A 104:6223–6228.

53. Kawauchi K, K Araki, K Tobiume and N Tanaka. (2008). p53 regulates glucose metabolism through an IKK-NF-kappaB pathway and inhibits cell transformation. Nat Cell Biol 10:611–618.

54. Carter KL, E Cahir-McFarland and E Kieff. (2002). Epstein-barr virus-induced changes in B-lymphocyte gene expression. J Virol 76:10427–10436.

55. Ak P and AJ Levine. (2010). p53 and NF-kappaB: different strategies for responding to stress lead to a functional antagonism. FASEB J 24:3643–3652.

56. Prasad SM, M Czepiel, C Cetinkaya, K Smigielska, SC Weli, H Lysdahl, A Gabrielsen, K Petersen, N Ehlers, et al. (2009). Continuous hypoxic culturing maintains activation of Notch and allows long-term propagation of human embryonic stem cells without spontaneous differentiation. Cell Prolif 42:63–74.

57. Bash J, WX Zong, S Banga, A Rivera, DW Ballard, Y Ron and C Gelinas. (1999). Rel/NF-kappaB can trigger the Notch signaling pathway by inducing the expression of Jagged1, a ligand for Notch receptors. EMBO J 18:2803–2811.

Address correspondence to:
Dr. Hiroyuki Moriyama
Pharmaceutical Research and Technology Institute
Kinki University
3-4-1 Kowakae
Higashi-Osaka
Osaka 577-8502
Japan

E-mail: moriyama@phar.kindai.ac.jp